NAVAL POSTGRADUATE SCHOOL
MONTEREY, CALIFORNIA

THESIS

OPTICAL MODULATOR LM 0202 P CHARACTERISTICS: APPLICATION TO AMPLITUDE MODULATION OF ARGON-ION LASER

by

Michael Christopher Ladner

June,1996

Thesis Advisor: S. Gnanalingam
Andres Larraza

Approved for public release; distribution is unlimited.

19960905 008

REPORT DOCUMENTATION PAGE

Form Approved OMB No. 0704-0188

Public reporting burden for this collection of information is estimated to average 1 hour per response, including the time for reviewing instruction, searching existing data sources, gathering and maintaining the data needed, and completing and reviewing the collection of information. Send comments regarding this burden estimate or any other aspect of this collection of information, including suggestions for reducing this burden, to Washington Headquarters Services, Directorate for Information Operations and Reports, 1215 Jefferson Davis Highway, Suite 1204, Arlington, VA 22202-4302, and to the Office of Management and Budget, Paperwork Reduction Project (0704-0188) Washington DC 20503.

1. AGENCY USE ONLY	2. REPORT DATE June 1996	3. REPORT TYPE AND DATES COVERED Master's Thesis
4. TITLE AND SUBTITLE OPTICAL MODULATOR LM 0202 P CHARACTERISTICS:APPLICATION TO AMPLITUDE MODULATION OF ARGON-ION LASER		5. FUNDING NUMBERS
6. AUTHOR(S) Michael C. Ladner		
7. PERFORMING ORGANIZATION NAME(S) AND ADDRESS(ES) Naval Postgraduate School Monterey CA 93943-5000		8. PERFORMING ORGANIZATION REPORT NUMBER
9. SPONSORING/MONITORING AGENCY NAME(S) AND ADDRESS(ES)		10. SPONSORING/MONITORING AGENCY REPORT NUMBER
11. SUPPLEMENTARY NOTES The views expressed in this thesis are those of the author and do not reflect the official policy or position of the Department of Defense or the U.S. Government.		
12a. DISTRIBUTION/AVAILABILITY STATEMENT Approved for public release; distribution is unlimited.		12b. DISTRIBUTION CODE

13. ABSTRACT

The purpose of this thesis is to examine the possibility of using a commercial elecro-optic modulator, the LM 0202 P modulator manufacured by Gsanger Opto-Elektroniks of Germany, to provide an amplitude modulated light source to test a theory of the conversion of amplitude to frequency modualtion of light in fiber optics. The main focus of this thesis is to experimentally determine the performance characteristics of the modualtor including the frequency response in the frequency range 1 kHz to 150 MHz. The effects of inductive loops, both external and internal to the modulator, are examined and solutions discussed. Amplitude modualtion of an Argon-Ion Laser operating at 514.5 nm at twenty-five percent modulation at 125 MHz has been achieved.

14. SUBJECT TERMS ELECTRO-OPTIC MODULATOR			15. NUMBER OF PAGES 85
			16. PRICE CODE
17. SECURITY CLASSIFICATION OF REPORT Unclassified	18. SECURITY CLASSIFICATION OF THIS PAGE Unclassified	19. SECURITY CLASSIFICATION OF ABSTRACT Unclassified	20. LIMITATION OF ABSTRACT UL

NSN 7540-01-280-5500

Standard Form 298 (Rev. 2-89)

Approved for public release; distribution is unlimited.

OPTICAL MODULATOR LM 0202 P CHARACTERISTICS: APPLICATION TO AMPLITUDE MODULATION OF ARGON-ION LASER

Michael C. Ladner
Lieutenant, United States Navy
B.S., United States Naval Academy, 1989

Submitted in partial fulfillment
of the requirements for the degree of

MASTER OF SCIENCE IN PHYSICS

from the

NAVAL POSTGRADUATE SCHOOL
June 1996

Author: _____
Michael C. Ladner

Approved by: _____
S. Gnanalingam, Thesis Advisor

_____
Andres Larraza, Thesis Advisor

_____
William Colson, Chairman
Department of Physics

ABSTRACT

The purpose of this thesis is to examine the possibility of using a commercial electro-optic modulator, the LM 0202 P modulator manufactured by Gsanger Opto-Elektroniks of Germany, to provide an amplitude modulated light source to test a theory of the conversion of amplitude to frequency modulation of light in fiber optics. The main focus of this thesis is to experimentally determine the performance characteristics of the modulator including the frequency response in the frequency range 1 kHz to 150 MHz. The effects of inductive loops, both external and internal to the modulator, are examined and solutions discussed. Amplitude modulation of an Argon-Ion Laser operating at 514.5 nm at twenty-five percent modulation at 125 MHz has been achieved.

TABLE OF CONTENTS

I. INTRODUCTION 1
II. OPTICAL MODULATOR LM 0202 P 7
A. INTRODUCTION 7
B. THEORY 8
C. APPLIED DC VOLTAGE PERFORMANCE 12
1. Experimental Set Up 12
a. Procedure 12
b. Component Alignment 16
2. Modulator Output 17
a. DC Characteristic Curve 17
b. Modulator Linearity 19
D. LOW FREQUENCY AC/DC VOLTAGE PERFORMANCE 21
III. RADIO FREQUENCY AMPLITUDE MODULATION 25
A. INTRODUCTION 25
B. RF TRANSFORMER 25
1. Introduction 25
2. Properties of the Transformer Secondary 27
3. Experimental Procedure 29
4. Results 31
C. PARALLEL TUNED CIRCUIT 32
1. Introduction 32
2. Experimental Procedure 33
3. Results 34
IV. RESULTS AND CONCLUSIONS 41
A. ANALYSIS OF RESULTS 41
B. CONCLUSIONS AND RECOMMENDATIONS 42

APPENDIX A LASER SPECIFICATIONS AND OPERATING PROCEDURES 45
APPENDIX B DATA 49
APPENDIX C COMPONENT SPECIFICATIONS 61

LIST OF REFERENCES 71

INITIAL DISTRIBUTION LIST 73

LIST OF FIGURES

1. Modulated Waves....2
2. Time Evolution of Modulation....4
3. LM0202 P Electro-optic Modulator....7
4. Typical Equipment Set-up for Modulator Use....9
5. Polarization Changes due to Applied Voltage Alone....10
6. Transmission Percentage as a Function of Applied Modulating Voltage....11
7. Test Circuit Diagram....13
8. Detector 1 Response Curve....13
9. Equipment Set-Up for DC Voltage Testing....15
10. Photograph of the Equipment Set-Up....15
11. Photograph of the Electro-Optic Modulator with Alignment Components....16
12. Applied DC Voltage to Optical Modulator....18
13. Linearity Response Circuit....20
14. Linearity Test of Internal Circuit of Modulator....20
15. Circuit Diagram for 1 kHz Testing....21
16. Representative outputs of modulator at 1 kHz and various voltages....22
17. Determination of Linear Response of Modulator....24
18. Equipment Setup for Transformer Action....26
19. Coil Dimensions....27
20. Equipment Set up....29
21. Microscope Slide Reflector....30
22. Detector 3 Calibration Curve....30
23. Parallel Tuned Circuit....33
24. Modulation Percentage vs. Frequency....35
25. Modulator Response....36
26. Setup....39

I. INTRODUCTION

Due to self-interaction effects, the frequency of a wave in a dispersive medium is amplitude dependent, and in the weakly nonlinear regime it is of the form

$$\omega(k) = \omega_0(k) + \omega_2(k)e. \tag{1.1}$$

In expression (1.1), $\omega_o(k)$ is the linear dispersion relation, $\omega_2(k)$ is the nonlinear coefficient, and e is the energy density which is proportional to the square of the wave amplitude. For the case of fixed frequency, positive group velocity, and $\omega_2 > 0$, the effect of nonlinearity is to decrease the wavenumber k as the amplitude of the wave field increases.

To understand the combined effects of dispersion and nonlinearity, we follow closely the physical argument given by Larraza and Coleman [1]. Consider an initial state of a modulated wave observed in a frame moving with the group velocity (Figure 1a). An observer in this frame would see the crests of the wave propagate. Because of dispersion, the group and phase velocities are different.

Consider now the case where the nonlinear coefficient $\omega_2 > 0$. An observer in the frame moving with the linear group velocity would observe bunching of the crests when the modulation amplitude is low and anti-bunching when the modulation amplitude is high (Figure 1b). For positive dispersion, $\omega''(k) > 0$,

$$\delta v_g = \omega''(k)\delta k \tag{1.2}$$

increases towards the troughs of the modulation. Dispersive effects cause the energy to approach the troughs of the envelope, and the modulation propagates. Thus, to an observer moving with the linear group velocity, the modulation is no longer stationary.

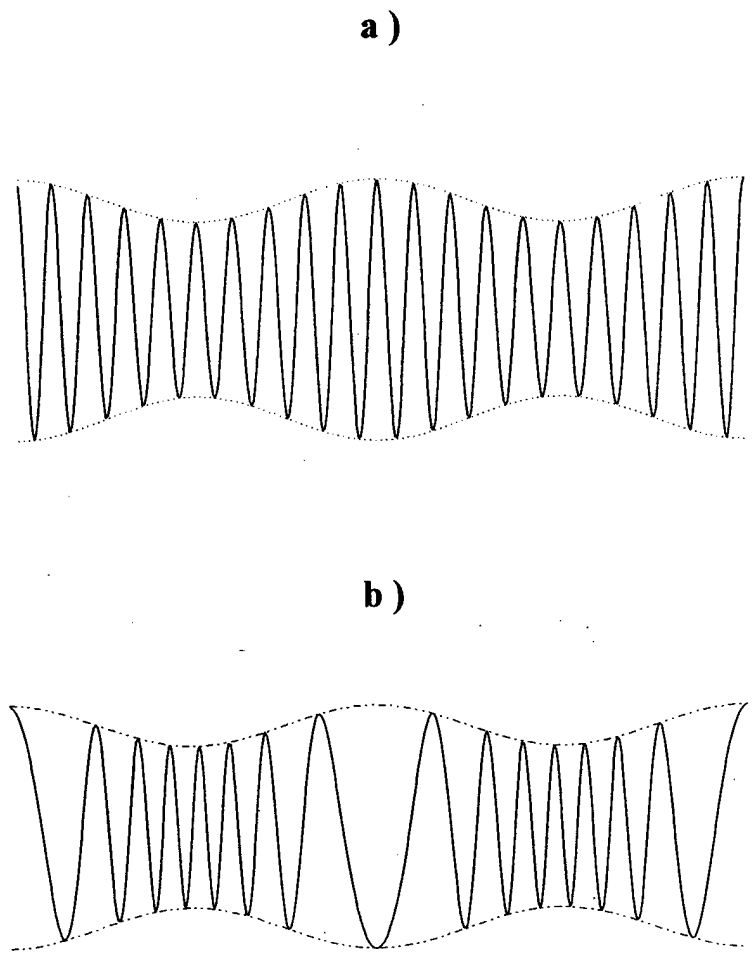

Figure 1. Modulated waves. a) Initial state of a modulated wave in the frame moving with the group velocity v_g. b) For positive dispersion, $\omega''(k)$ >0 and $\omega_2 > 0$, δv_g increases toward the troughs of the modulation and the modulation propagates.

Instead, the modulation can propagate with both a velocity that is either higher or lower than the linear group velocity. This result is general when the product $\omega_2\omega''$ is positive.

The stability of the modulation has the important consequence of AM-FM conversion. This effect can be physically understood by considering again a modulated wave in a frame moving with the linear group velocity (Figure 2a). Assume that both the dispersion and the nonlinear coefficient ω_2 are positive. Due to nonlinear effects, an observer at a fixed location in this frame would see, after some time, alternating bunching and anti-bunching of the wave crests (Figure 2b). Because dispersive effects cause the energy to approach the troughs of the envelope, for this observer it would appear that at some time later the initial amplitude modulation has become a frequency modulation (Figure 2c). Dispersive effects would again remove energy from the region where the crests are more spread apart to the region where the crests are closer together. For the observer fixed in the frame moving with the group velocity it would appear that an amplitude modulation is superimposed upon the frequency modulated signal (Figure 2d). Nonlinearity will prevent an overshoot of energy flow to the crest of the modulation, and an amplitude modulation 180° out of phase with respect to the original signal results at a later time (Figure 2e). In the frame moving with the group velocity, the process repeats periodically, and an observer in this frame sees that the modulations experience beats. In the laboratory frame if a source is generating an amplitude modulated signal, some distance away it will become frequency modulated. Larraza and Coleman [1] also give a quantitative theory for this effect. They have shown that an amplitude modulated signal with amplitude $\sqrt{e_0}$, modulation amplitude m, modulation frequency Ω, and carrier frequency ω will evolve according to

$$a(x,t) = \sqrt{e_0}\left[1 + m\cos(\Delta x)\cos(\Omega t - \eta x)\right]$$
$$* \ \cos\left[k_0 x - \omega t - \frac{2m\omega_o'}{\Omega}\sqrt{\frac{\omega_2 e_0}{\omega_o''}}\ \sin(\Delta x)\cos(\Omega t - \eta x)\right], \qquad (1.3)$$

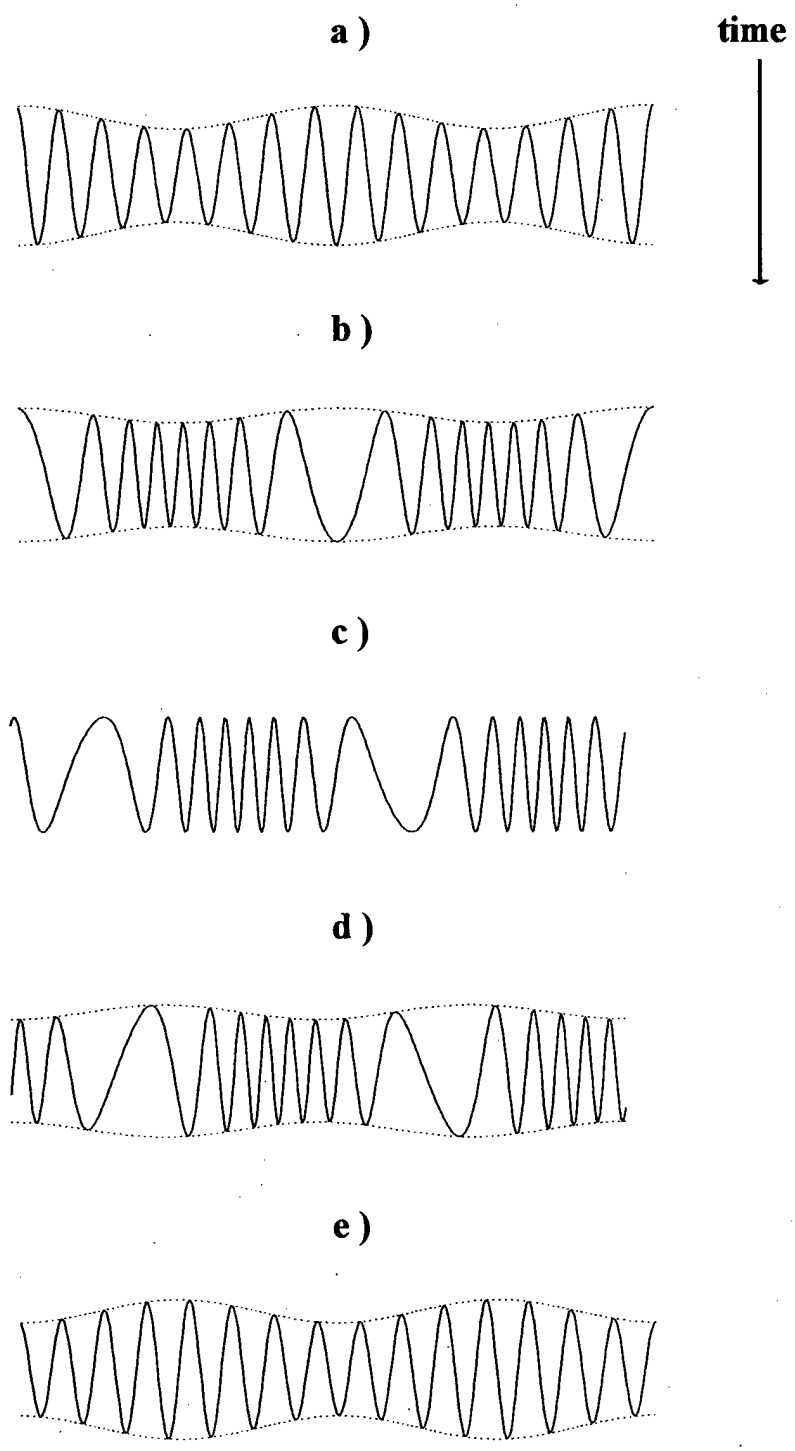

Figure 2. Time evolution of modulation. An observer in a frame moving with the linear group velocity observes AM–FM conversion in time.

where $\Delta = \Omega\sqrt{\omega_0'' \omega_2 e_0} / \omega_0'^2$.

A possible application of this result is broadband tunable lasers using fiber optics. Here, we are interested in single mode fibers consisting of a glass core of high index of refraction surrounded by a cladding with a lower index of refraction (about 0.1% smaller). In this case, for light in the visible range the dispersion is normal with $\omega_o''(k) < 0$. For light with intensity I, the index of refraction is given by $n(I) = n_0(\omega) + n_2 I$, where $n_o \approx$ 1.5. Thus, the frequency nonlinear coefficient $\omega_2 \approx -\alpha n_2 \omega_o / n$ is negative, where α is a numerical factor of order unity. The order of magnitude of the coefficient n_2 (in units of cm^2/W) is about 10^{-11} or higher in doped glasses.

Because the product $\omega_o''(k)\omega_2 > 0$, the physical picture presented above applies to this case. In particular, for a 0.1 W source operating at a frequency of 5.8×10^{14} Hz and a 50% amplitude modulation of 10^{10} Hz in a 10 μm^2 fiber, the distance $x_m = \pi/2\Delta$ for AM–FM conversion is about 20 m in doped glasses. The corresponding FM frequency spectrum has a range of about 3.5×10^{14} Hz in doped glasses. Thus, in doped glasses, an amplitude modulated green light alternating between bright and dim at the source will alternate between red and blue at a rate of 10^{10} Hz at a location about 20 m down the fiber. This mechanism allows the possibility of producing tunable phased–locked coherent light from a single frequency coherent source.

The purpose of this thesis is to examine one means of amplitude modulating an Argon-Ion laser operating at 514.5 nm using a commercially available electro-optic modulator. This thesis will specifically examine the characteristics of the LM 0202 P electro-optic modulator manufactured by Gsanger Opto-Elektroniks of Germany. The

manufacturer has provided very limited operational data with the modulator for the frequency range (10-150 MHz) and the modulation percentage that will be required for the purpose of proving the AM-FM conversion theory just covered. The limited data available is understandable because the usual applications of an intensity modulator operate in the regime of a few hundred kilohertz. Gsanger has claimed to have laboratory tested the modulator in our frequency range and found a flat response at 1 volt modulating voltage from zero to 150 MHz. However, as this only corresponds to approximately two percent modulation, we will attempt to test it at full modulation. Gsanger has claimed to test the modulator at full intensity modulation, but only up to a frequency of 20 MHz.

This thesis will provide new data for the characteristic response of the modulator for the full frequency range of 150 MHz at as high a range of modulation as possible. Limited in resources compared to a commercial laboratory, we will also develop the driving circuit power requirements, and test the circuits, detectors, power supplies and amplifiers required to modulate the laser beam at the highest frequency possible.

II. OPTICAL MODULATOR LM 0202P

A. INTRODUCTION

As discussed previously, the electro-optic modulator LM 0202 P will be investigated to determine its operating characteristics at various applied AC voltages to provide an amplitude modulated laser light source for the purpose of testing AM-FM conversion in optical fibers.

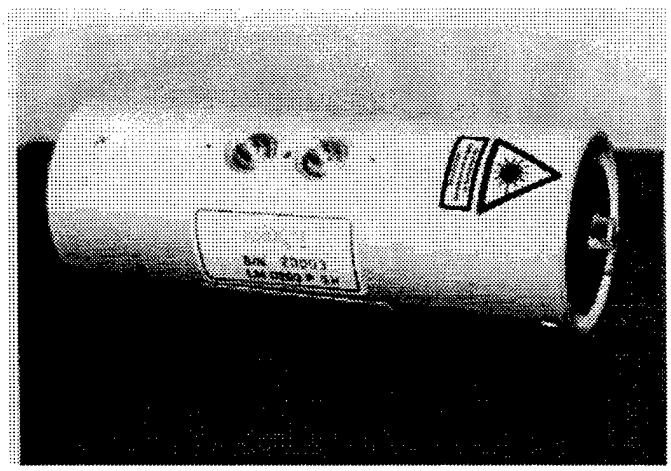

Figure 3. LM0202 P Electro-optic Modulator. A Brewster crystal is mounted on the downbeam (right) end. The SMC connections on the side are to provide for applied AC and DC voltages to the internal crystals. The modulator can handle 0.1 - 5 W of optical power in the 250 - 1100 nm wavelength range. The input aperture is 3 x 3 mm with overall dimensions of 50 mm diameter and 138 mm length.

We first determine the basic transmission characteristics at DC. Then, we add an AC voltage source in series at discrete amplitudes and frequencies. This chapter will cover the theory of modulator operation, its basic DC characteristics and its behavior when DC voltage is placed in series with low frequency AC voltages. This is to verify manufacturer characteristics and establish operating parameters which are used for higher frequencies. Application of the higher frequency AC voltages and the various circuits required to handle

their high power requirements and shorter detector response times will be covered in the next chapter.

B. THEORY

An electro-optic modulator can be used to control the polarization state of an optical beam electrically. As will be explained, controlling the polarization of a laser light source can lead to amplitude modulation of the laser beam without direct modulation of the laser. This will ensure that no degradation occurs to the laser stability and power output.

The essential element of any electro-optic modulator is the crystal, usually several, mounted optically in series and electrically in parallel. It has two principal axes, conveniently labeled x' and y'. Light incident on the crystal can be separated into two components, one along each axis.

The index of refraction along these axes may be controlled via application of a force field, i.e., electrical, magnetic, or mechanical. Specifically, an electric field applied across the optical medium redistributes the electrons within it to distort the polarization and hence the refractive index of the medium. The electro-optic effect is the change in the indices of refraction of a medium (i.e., a crystal) caused by that electric field. The change in refractive index as a function of the applied electric field, E, can be obtained from an equation of the form [2]:

$$\Delta\left(\frac{1}{n^2}\right) = rE + PE^2, \tag{2.1}$$

where r is the linear electro-optic coefficient and P is the quadratic electro-optic coefficient. The linear variation is known as the Pockels effect and the quadratic term is called the Kerr

effect. Assuming a small Kerr effect, the new refractive indices along the principal axes become [2]:

$$n_{x'} = n_o + \frac{n_o^3}{2} r E_z, \qquad (2.2)$$
$$n_{y'} = n_o - \frac{n_o^3}{2} r E_z,$$

The crystal in the LM0202P is potassium dideuterium phosphate KD_2PO_4 or KD*P. KD*P has a negligible Kerr effect. Since the speed of light in the medium is inversely proportional to the index of refraction, n, by the relation [3]

$$v = c / n \qquad (2.3)$$

where v is the speed of light in the medium and c is the speed of light in vacuum, the speed of light is also affected by the application of an electric field.

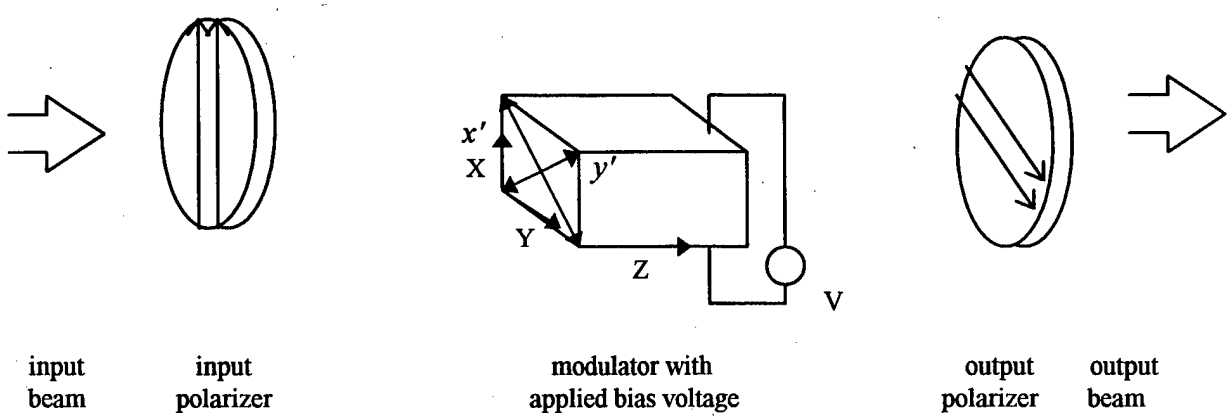

Figure 4. Typical Equipment Set-up for Modulator Use. The total phase delay is equal to the sum of the natural phase delay of $\pi/2$ and the induced delay caused by the electric field. [4]

Therefore, it can be seen that through application of an electric field (typical setup seen in Figure 4), the speed of propagation of the light along the axis is changed resulting in a change in the optical pathlength for each component. We define Γ as the difference in phase

delay between the two linear wave components that emerge from the crystal. The amount of phase delay that a monochromatic wave acquires from traveling through the crystal is related to its speed (or index of refraction), wavelength and the path length, L, inside the crystal.

With no voltage applied to the modulator, it behaves like a quarter-wave plate in that it changes linearly polarized light to circularly polarized light at a particular wavelength. This is because of a proprietary compensation scheme that Gsanger has developed using the four matched crystals in the modulator to take advantage of the natural birefringence of the KD*P crystal. Initially, a vertically polarized beam incident at 45° to the principal axes of the crystal will yield two components of equal amplitude with a Γ of $\pi/2$, and thus be circularly polarized. As voltage is applied to create the electric field, the electro-optic effect changes Γ (seen in Figure 5). This is because the indices of refraction change according to equation 2.2 and thus the optical pathlengths also change. The phase delay between components is equal to the sum of the natural phase delay of $\pi/2$ and the induced delay caused by the electric field. The phase delay can be changed so that the linearly polarized incident beam can be changed to any polarization desired. With the help of a polarizer set perpendicularly to the incident light polarization and mounted at the output of the modulator, the intensity of the light source can be changed from full transmission to extinction.

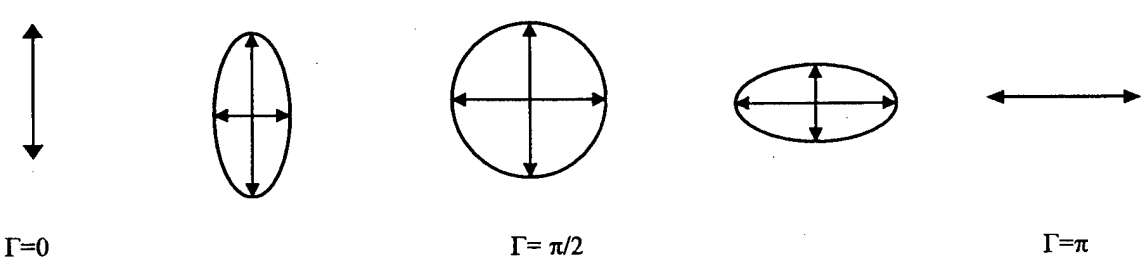

Figure 5. Polarization Changes due to Applied Voltage Alone. As the phase delay increases, the polarization can be changed from vertical to circular to horizontal. This process continues until the polarization is changed again to vertically polarized. [4]

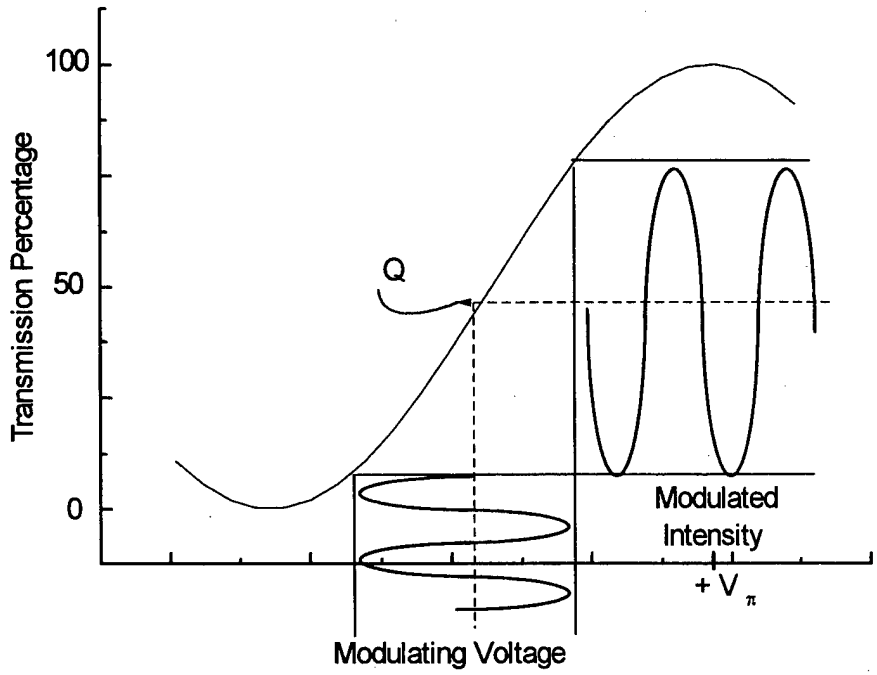

Figure 6. Transmission Percentage as a Function of Applied Modulating Voltage. Q marks the value midway between full transmission and extinction points. V_π is the full transmission voltage.

Amplitude Modulation may be obtained via an intensity modulator which incorporates the concepts explained above. Using a polarizer (or Brewster cube) at the output of the modulator as a horizontal polarizer, the transmission will vary from full extinction to full transmission. As can be viewed in Figure 6, if the applied modulating voltage is oscillating about the 50 percent transmission point, Q, an approximately sinusoidal amplitude modulated output can be developed from a continuous wave source.

Some limitations of electro-optic modulators are thermal drift and residual amplitude modulation. As researched by New Focus, Inc. [5], these effects must be taken into account when using an electro-optic modulator. Thermal drift occurs because of the temperature dependence of the crystals birefringence. Birefringence crystals have different indices of

refraction for each axis. Thermal drift is controlled by the LM0202 modulator by using four equal-length crystals placed optically in series. The thick aluminum housing also provides good thermal and mechanical stability. Residual amplitude modulation is induced by back reflections inside the modulator. These produce an unwanted amplitude modulation component. Residual amplitude modulation can be reduced by carefully aligning the beam down the center of the modulator. The actions taken to reduce this phenomenon are covered in the section on Component Alignment.

C. APPLIED DC VOLTAGE PERFORMANCE

The first step in achieving an amplitude modulated signal out of the modulator is to determine the DC transmission curve as shown in Figure 6. Once this curve is established for this modulator, the extinction/transmission voltages and the DC bias voltage offset can be determined. We used a Class 3b 300 mW vertically polarized continuous wave (CW) Argon-Ion Laser which operates at 514.5 nm. Specific laser characteristics and operating procedures may be found in Appendix A.

1. Experimental Set-Up

a. Procedure

To determine the points on the transmission curve, a DC voltage was applied to the modulator making use of the circuit shown in Figure 7. At DC, the electric circuit required to determine the transmission curve is quite simple and is essentially just a DC power supply in series with the modulator. Applied DC voltage data is recorded with a Keithley Digital Multimeter in parallel with the power supply and the modulator.

The laser is carefully aligned with the modulator and is set for an output of about 100 mW. The exact value can be changed up to a maximum of about 280 mW with the laser power supply that we have. The exact power setting of the laser is not that critical as long as

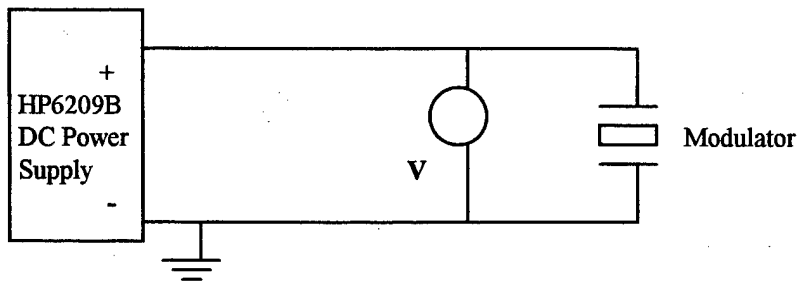

Figure 7. Test Circuit Diagram.

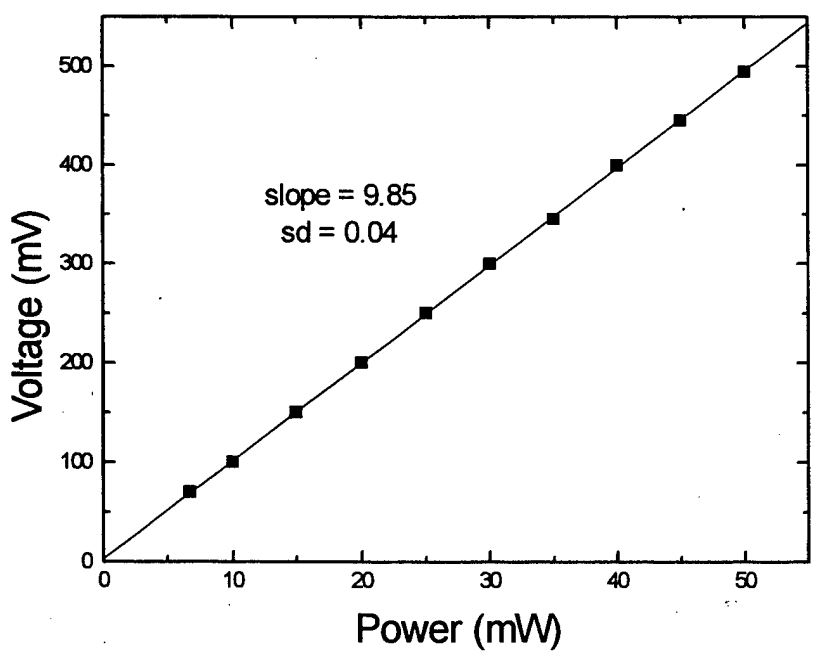

Figure 8. Detector 1 Response Curve. The voltage is measured with an oscilloscope from the analog output of the detector. Power is controlled via the laser power supply.

it does not exceed the saturation power limit of the photodetectors. The alignment procedures and techniques are covered later in this chapter. The output is measured using filtered silicon diode photodetectors connected to Newport Series 85 power meters. The meters also have an analog output coaxial connector in the back which provides a 1.999 volts full scale output. Figure 8 is a plot of the analog output voltage versus optical power as indicated by digital readout. The analog outputs are then connected to a Tektronix 2445A oscilloscope for analysis. More specifications for the Newport Power Meters and photodetectors are given in Appendix C.

As pictured in Figures 3 and 11, there is a Brewster cube mounted on the downbeam end of the modulator. This cube acts like the analyzer discussed in the theory of modulator operation section. Two detectors were used to measure the two components as shown in Figure 9. It is explained later why the behavior of both components must be understood even though only the horizontally polarized component will be eventually launched into a fiber optic cable in an effort to prove the AM-FM conversion theory. The Brewster cube separates the outgoing beam into horizontally and vertically polarized components. Using a variable angle linear polarizer, it was determined that the horizontal component was incident on Detector 1 and the vertical component was incident on Detector 2.

The modulator is shown as a capacitor in the circuit diagram because of its characteristic electronic performance. Its value is measured to be 82 pF with a BK Precision LCR meter.

We performed the experiment with both a floating and a grounded DC voltage source. As shown in Appendix B, there was no change in output based on whether the DC voltage was grounded or not. Thus, all experiments could be performed with a grounded DC source.

When the modulator is aligned properly, vertically polarized laser light oriented 45 degrees from the principal axes of the modulator, will become circularly polarized out of the modulator when there is no voltage applied to the LM0202 modulator. Thus, the two

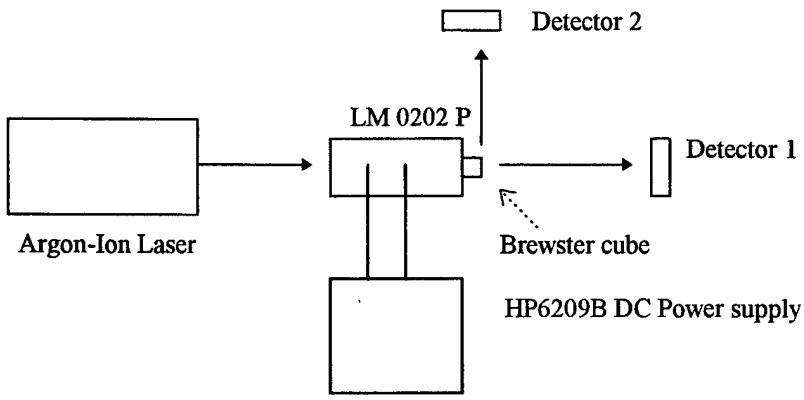

Figure 9. Equipment Set-Up for DC Voltage Testing. The Brewster cube separates the output into a horizontal component which travels to Detector 1 and a vertical component which travels to Detector 2.

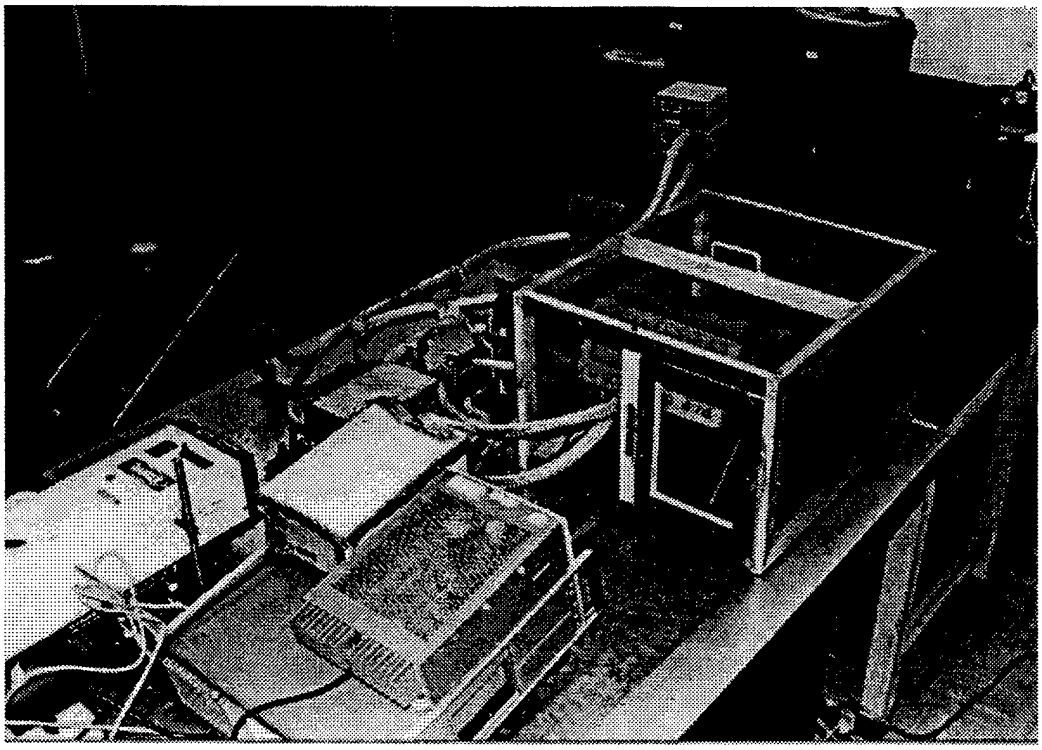

Figure 10. Photograph of the Equipment Set-Up.

(a)

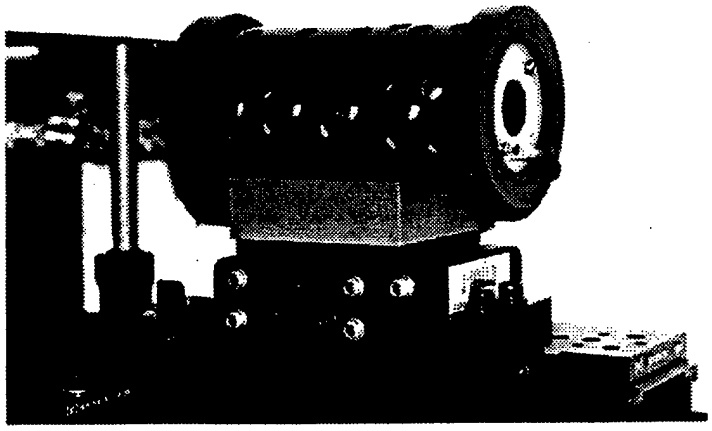

(b)

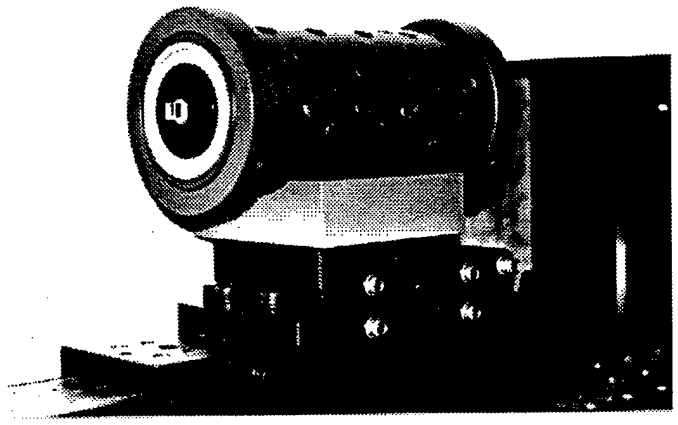

Figure 11. (a-b). Photographs of the Electro-Optic Modulator with Alignment Components. (a) View of the input to the modulator. (b). View of the downbeam end with the Brewster Cube. The plastic cuff is used to control the azimuthal rotation of the modulator while the 9082 Five Axis Aligner is used to align the modulator to the laser beam along the z axis.

components will be equal in amplitude at this point. This provides a check that the modulator is properly aligned. Once the transmission curve is known, the alignment can be checked at the 50 percent transmission point as well as the extinction and full transmission points.

b. Component Alignment

Proper alignment of components is by far the most difficult task and the greatest factor in affecting the accuracy of test results. Essentially only the laser and the modulator need to be aligned but eventually the laser light will also have to be launched into a fiber optic cable. Also the detectors used have various numerical apertures, some of which require exacting alignment standards.

The laser is placed on two lab jacks to control the angle of the beam into the modulator. The modulator itself required a special platform that starts with a 9082 Five Axis Aligner from New Focus Inc. It is a platform that can be mounted on an optical bench rail and has 5 allen wrench adjustment screws, to provide translational movement in the horizontal plane and rotational movement about horizontal and vertical axes. A schematic of the New Focus Aligner is provided in Appendix C. There is also the angular rotation in the azimuthal direction which has to be controlled to microradian accuracy to align the polarization of the incoming beam so that it is 45° to the principal axes of the crystals in the modulator. A special rotating cuff incorporating a micrometer adjuster, designed and machined in the Physics workshop, was attached to the modulator to set the azimuthal angle. This cuff can be seen in Figures 10 and 11.

2. Modulator Output

a. DC characteristic curve

The DC characteristic curve for the LM0202 modulator is shown in Figure 12. The laser output is set to approximately 75 mW. With a maximum tested transmission through the modulator of 94.8 percent, the power of each component was about 70 mW at full transmission. This power level is directly proportional to the laser output power. Increasing the laser power through the modulator only increased the amplitude of the curve, not its

general shape and voltage characteristics. This is why the laser output power is not remarkable at this point in the thesis.

Several facts can be derived from this curve. First, with no voltage applied to the modulator and with proper alignment, the vertically polarized laser beam becomes circularly polarized by the modulator as evidenced by the fact that the horizontal and vertical components are equal. As voltage is applied, the phase delay between the components change and the horizontal and vertical components are changed accordingly. The horizontal

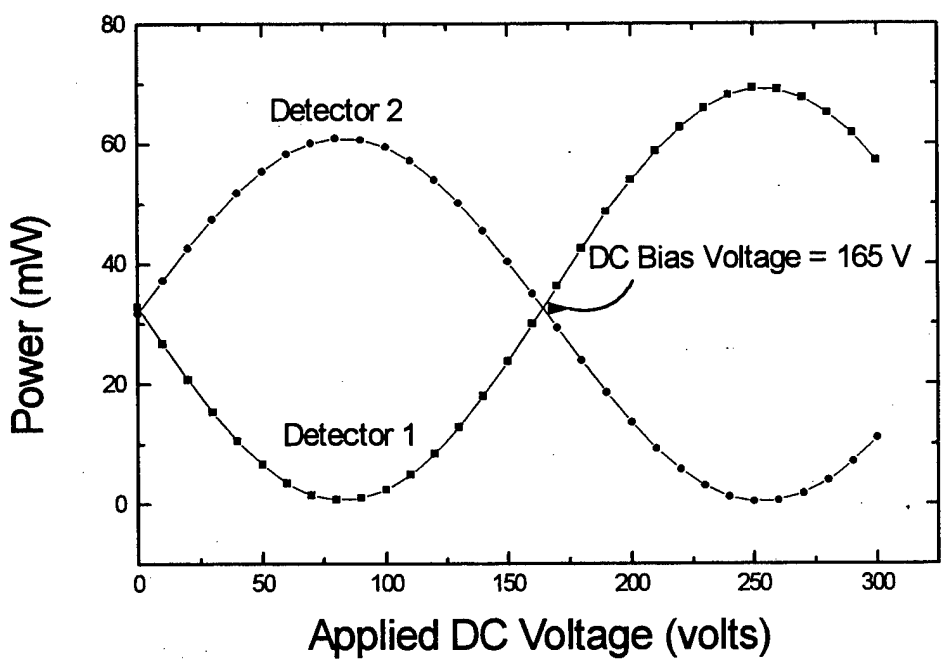

Figure 12. Applied DC Voltage to Optical Modulator. Notice that the Q point is at 165 volts and that the horizontal and vertical components are equal at 0 and 165 volts. The curve continues sinusoidally for the negative voltages. Reversing the voltage polarity at the modulator reverses the order of the extinction / transmission points for both components.

component (Detector 1) is extinguished at 80 volts and reaches full transmission at 255 volts. The vertical component (Detector 2) reacts inversely to the horizontal component at the same

voltage values. At 165 volts, the two components are of equal amplitude again. The 165 volt point is the Q point mentioned in the theory section about which the oscillating voltage will be applied. Therefore, an AC signal of 80 volts peak voltage in series with a DC supply set at 165 volts will cause the forward component to oscillate from zero amplitude to maximum amplitude at the frequency of the AC signal. This should result in an amplitude modulated output from a steady CW laser input.

It also has been determined that reversing the voltage leads to the inversion of the characteristic curve but not its shape. This means that the horizontal component reaches full transmission while the vertical component extinguishes at 80 volts and the reverse happens at 255 volts. With no DC bias, the curve can be reflected about the zero voltage axis. This means that the applied voltage can be oscillated with no DC offset and the same results can be achieved. Note that in this configuration, the slope of the horizontal component is opposite to that using a DC offset. It has been experimentally determined that ambient room temperature can change the 165 V equal amplitude point by a few volts due to crystal expansion and contraction.

b. Modulator Linearity

To check that the internal circuit of the modulator also provided a linear response to applied AC voltage, a current vs. AC voltage curve was measured. A transformer was used to step up the voltage from a function generator. The transformer used is the same transformer that will be used in Part D of this chapter. Circuit current can be derived from the voltage across R_1. At this frequency, the modulator has a reactance of 1.59 MΩ. The external resistor in series with the modulator was chosen to be small in comparison to the 1.59 MΩ, so that the current in the circuit was determined entirely by the internal modulator circuit. The

actual value of the resistor used was 15 kΩ. It can be seen that the internal circuit of the modulator performs linearly for the entire range of applied voltage which will result in full transmission to extinction.

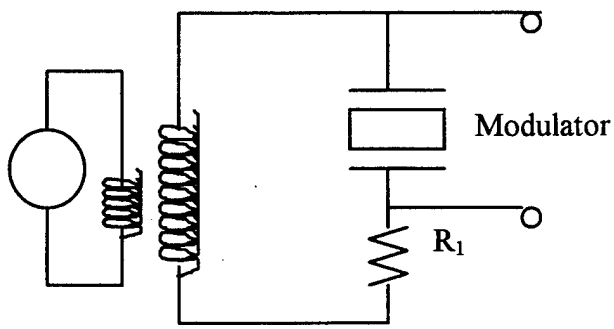

Figure 13. Linearity Response Circuit.

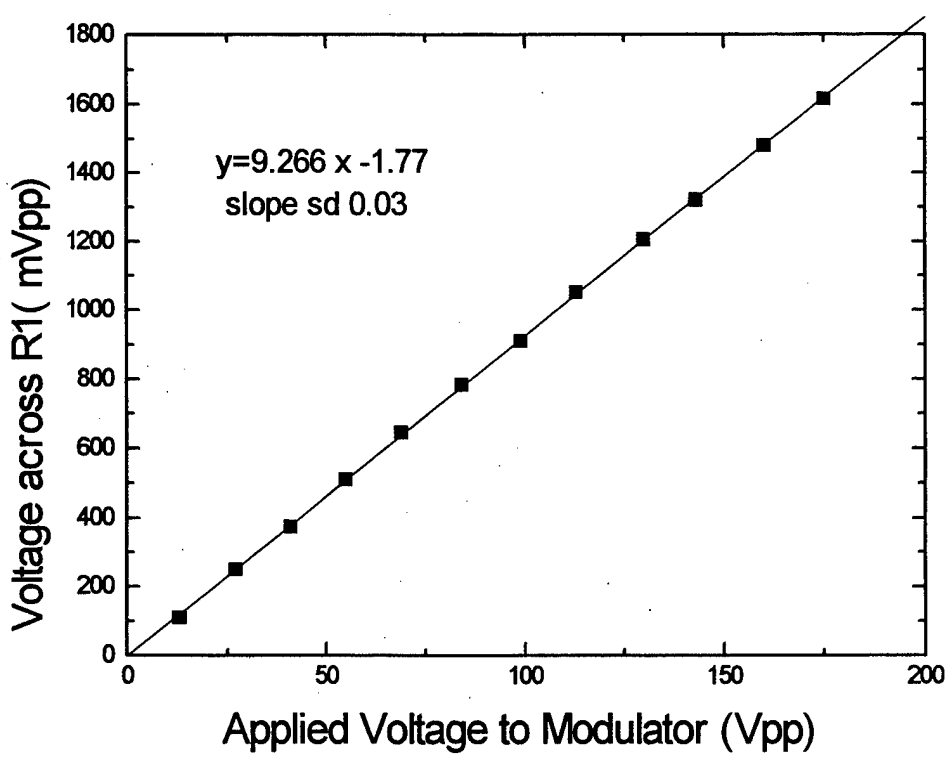

Figure 14. Linearity Test of Internal Circuit of Modulator.

D. LOW FREQUENCY AC/DC VOLTAGE PERFORMANCE

The next step in evaluating the modulator characteristics was to determine if a low frequency AC signal in series with the DC bias voltage would indeed result in amplitude modulation of the laser source. This first step was performed at 1000 Hz to stay within the bandwidth of the photodetectors. The circuit diagram was modified to add a resistor of

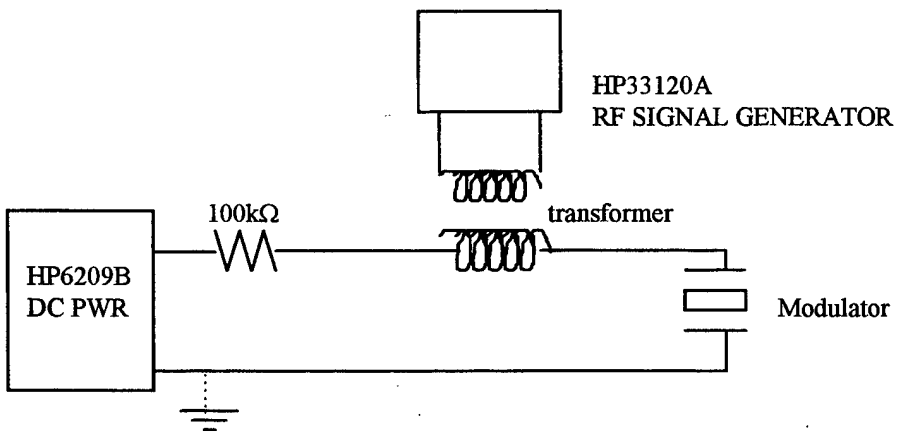

Figure 15. Circuit Diagram for 1 kHz Testing.

primary pk V	primary pp V	secondary pp V	range of voltage applied to modulator
1	2	28	151 - 179
2	4	57	137 - 194
3	6	82	124 - 206
4	8	112	109 - 221
5	10	138	96 - 234
6	12	168	81 - 249
7	14	198	66 - 264
8	16	228	51 - 279
9	18	256	37 - 293
10	20	284	23 - 307

Table 1. Transformer Characteristics and Applied Modulator Voltage at 1 kHz. It can be seen that full Modulation is attained at 5.7 Vp applied to the primary of the transformer.

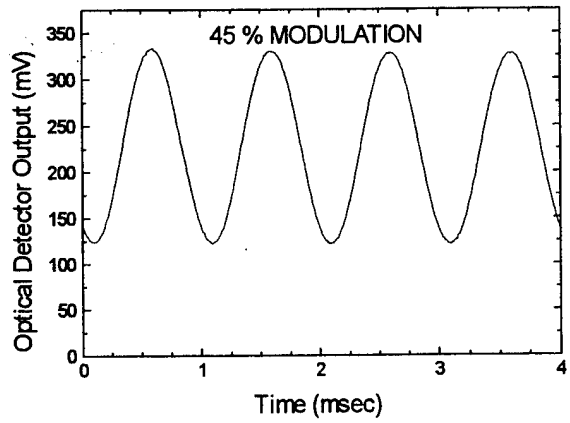

(a)

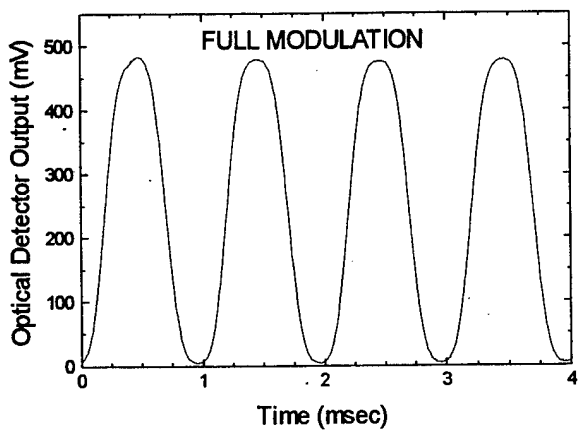

(b)

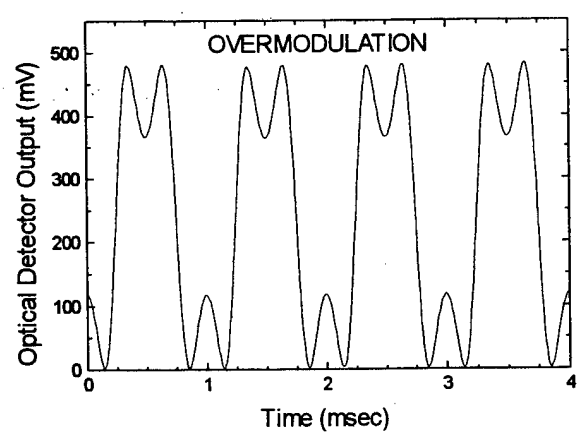

(c)

Figure 16. Representative outputs of modulator at 1 kHz and various voltages. Shown are optical detector outputs for secondary AC voltages (a) 57 V_{pp} (b) 165 V_{pp} (c) 284 V_{pp}.

100 kΩ to protect the DC power supply against an accidental short circuit, and the transformer required to step up the AC signal generator voltage was in series with the modulator.

The transformer used is a filament transformer manufactured by Triad Transformer Corp. Its specifications are provided in Appendix C.

Note that in Figure 16 and Table 1, full modulation of the laser output is obtained at 1 kHz when the secondary AC voltage is 165 V_{pp}. The amount of modulation can be controlled by the amount of AC voltage applied to the primary of the transformer coil. Modulation above approximately fifty percent is not linear as this exceeds the near linear portion of the DC characteristic curve in Figure 12. This effect is easily seen in plots c and d of Figure 16 above. Notice that the maximum amplitude does not increase past that achieved at full modulation, only the shape of the waveform distorts as more voltage is applied. The linear response portion of the modulator is shown in Figure 17. The response is linear until the AC voltage applied to the modulator reaches about 75 V_{pp}.

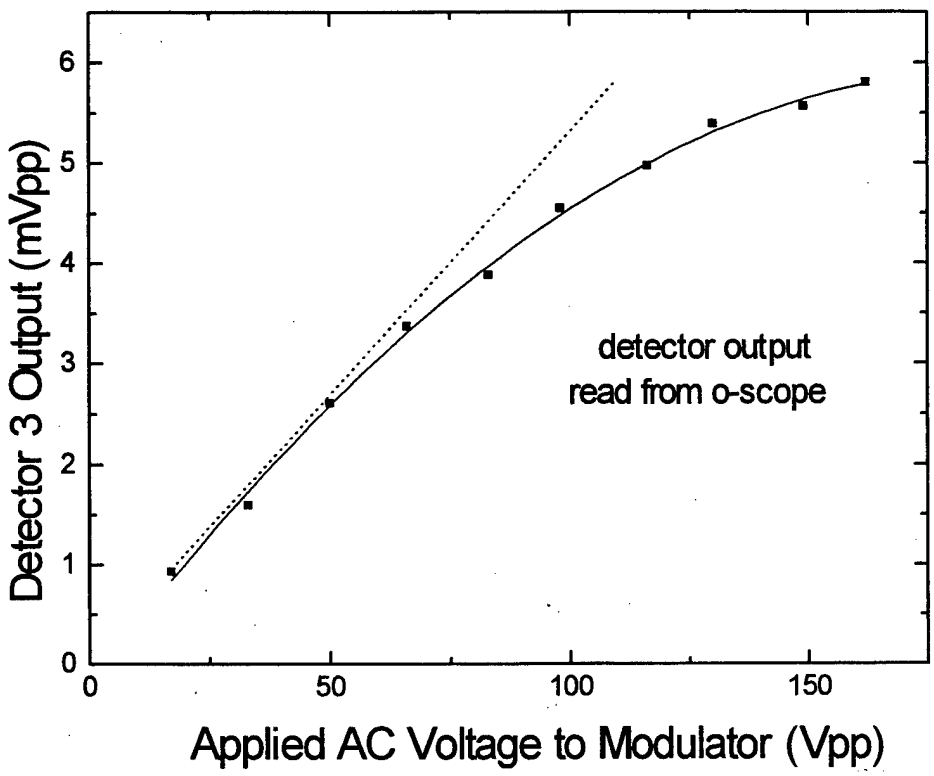

Figure 17. Determination of Linear Response of Modulator.

III. RADIO FREQUENCY AMPLITUDE MODULATION

A. INTRODUCTION

It has already been stated that the ultimate goal of the experiment was to obtain maximum amplitude modulation at the highest possible frequency so as to minimize the length of the fiber-optic cable needed to achieve conversion from amplitude modulation to frequency modulation. The purpose of this chapter is to describe the circuits that were designed and tested to drive the modulator at frequencies from 10 MHz to 150 MHz, with voltages up to 160 V_{pp}.

B. RF TRANSFORMERS

1. Introduction

The modulator is basically a crystal with two electrodes attached to it. It was therefore assumed that the electrical behavior of the device was similar, if not identical, to that of a capacitor. The capacitance was measured with a BK LCR meter and found to be 82 pF. Since the reactance of this capacitance is only 13 ohms at 150 MHz, it was evident that useful modulating voltages would not be obtained by connecting the modulator directly to the output terminals of a typical radio frequency (RF) signal generator or RF amplifier. Such devices generally need a 50 ohm load resistance for maximum power transfer, or a higher load impedance for maximum output voltage. Furthermore, the available signal generators had a maximum open-circuit output voltage of only 20 V_{pp}. So it was decided to drive the modulator through a tuned radio frequency transformer with both the primary and secondary circuits tuned to the working frequency.

It turned out, however, that the Q-factor of the secondary circuit was not sufficiently high to boost the output voltage to 160 Vpp, and it became necessary to make use of a RF amplifier to enhance the voltage supplied by the signal generator. The experimental arrangement used to drive the modulator is shown in Figure 18. Note that it includes

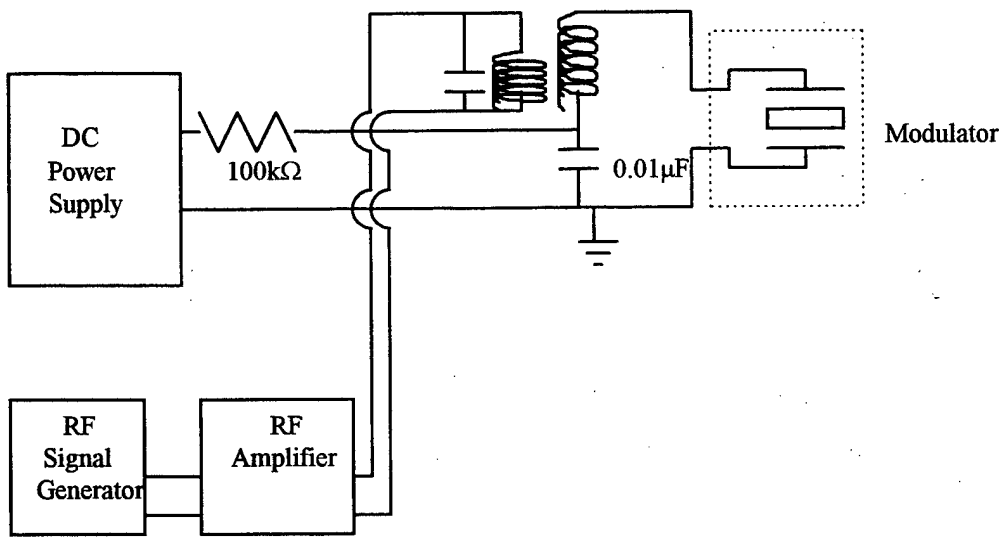

Figure 18. Equipment Setup for Transformer Action.

provision for applying a DC voltage to the modulator in addition to the RF voltage. This allows the adjustment of the bias voltage to ensure that the modulator operates at the 50% transmission point for symmetrical modulation (see section C of Chapter I). The purpose of the 0.01μF capacitor is to ensure that the bottom end of the secondary is at AC ground while being at an elevated DC voltage. The 100 kΩ resistor protects the DC power supply from an accidental short circuit.

Separate transformers were wound with different numbers of secondary turns to resonate at different frequencies. They were tested with an 82 pF capacitor before being used

to drive the modulator. In each case, the number of primary turns was adjusted for maximum secondary voltage at resonance. Satisfactory results were obtained up to 20 MHz. Above that frequency, however, a transformer could not be used because the required number of turns in the primary and secondary windings was so small that there was a severe mismatch between the primary impedance and the output impedance of the amplifier. The transformer was therefore replaced by a parallel tuned circuit. This is discussed in Section C of this chapter. The characteristics of the secondary winding of one of the transformers are discussed in the next section.

2. Properties of the Transformer Secondary

The resonance frequency f_o of an RLC circuit is [6]

$$f_o = \frac{1}{2\pi\sqrt{LC}}. \tag{3.1}$$

For a fixed capacitance C, the higher the frequency, the smaller is the inductance, L, and consequently the smaller is the number of turns required to obtain resonance. The required

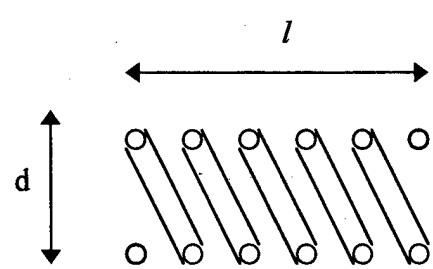

Figure 19. Coil Dimensions. Length of coil, l, diameter of coil, d, radius of coil, r = d/2, number of turns, N.

number of coils, N, for a required inductance, L, is given by [7]

$$N = \left({L(\mu H)}/{Fd} \right)^{1/2} \tag{3.2}$$

where F is a form factor which is a function of the ratio of d/l, where d is the diameter of the coil; and l is the length of the coil. It is important to realize that in this section, all length dimensions are measured in *inches*. The form factor F is given in a figure in reference 7, p. 6-1. Inductance then can be calculated to an accuracy of approximately one percent by [7]

$$L = n^2\left(r^2/9r + 10l\right) \quad \mu\text{H}. \tag{3.3}$$

Here, r is the radius of the coil, not the radius of the wire. Inductor coils were made from fourteen, sixteen, and eighteen gauge enameled copper wire with the following results for 10 MHz resonant frequency:

	14 gauge	16 gauge	18 gauge
n	42	47	44
L_{meas} (μH)	2.70	2.75	2.79
L_{calc} (μH)	2.03	2.40	2.60
Q	56	30	25
f_o (MHz)	11.6	9.95	10.2
wire diameter	0.0641	0.0524	0.0418
coil diameter	0.318	0.318	0.318
length of coil	3.0	2.5	2.25
F, form factor	0.0031	0.0035	0.0029

Table 2. Inductor Properties for 10 MHz resonance frequency.

The inductance of the secondary was measured with a HP 4194A Impedance / Gain-Phase Analyzer. The primary was not wound at the time of measurement. Fourteen gauge enameled copper wire was selected for the secondaries of all transformers tested.

3. Experimental Procedure

DC alignment was accomplished as discussed in Chapter II with Detectors 1 and 2 reading approximately 30 mW with 168 V DC bias. Modifications to the equipment setup were also required in order to analyze the output of the modulator. The Newport detectors, previously used for Detectors 1 and 2, only had a bandwidth of 180 kHz. The detector used for higher frequencies, shown as Detector 3 in Figure 20, was a Opto-Electronic Series PD30-03 avalanche-type silicon diode photodetector. It has a specified bandwidth of 1 GHz and

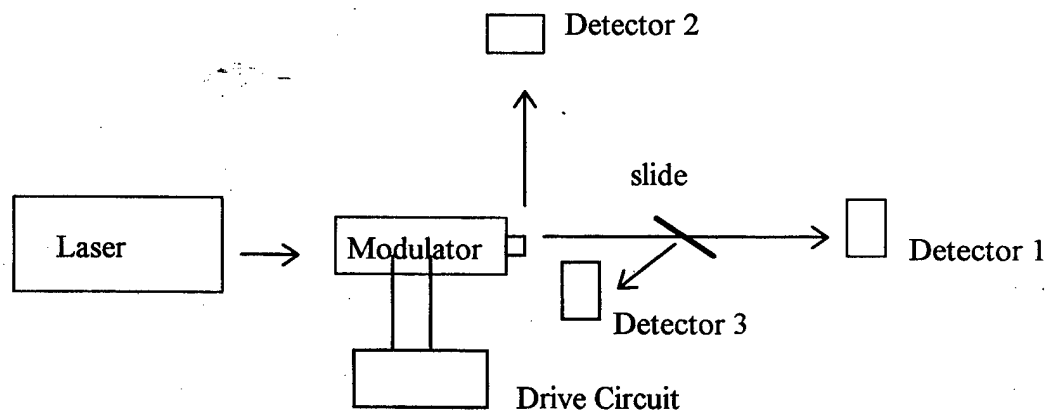

Figure 20. Equipment Set up.

was tested in the lab and found to provide a response beyond 250 MHz. The detector's diode current limit of 200 μA corresponded to an optical power of approximately 4 mW. Therefore, it could not take the full range of power that the laser was capable of putting into Detectors 1 and 2. So, a standard microscope slide was used to reflect a low percentage of the power into Detector 3. The slide has been experimentally tested to provide approximately five percent reflection. This works out to be about 1.5 mW out of 30 mW incident on Detector 1. The device used to aim the reflection into Detector 3 is shown in Figure 21.

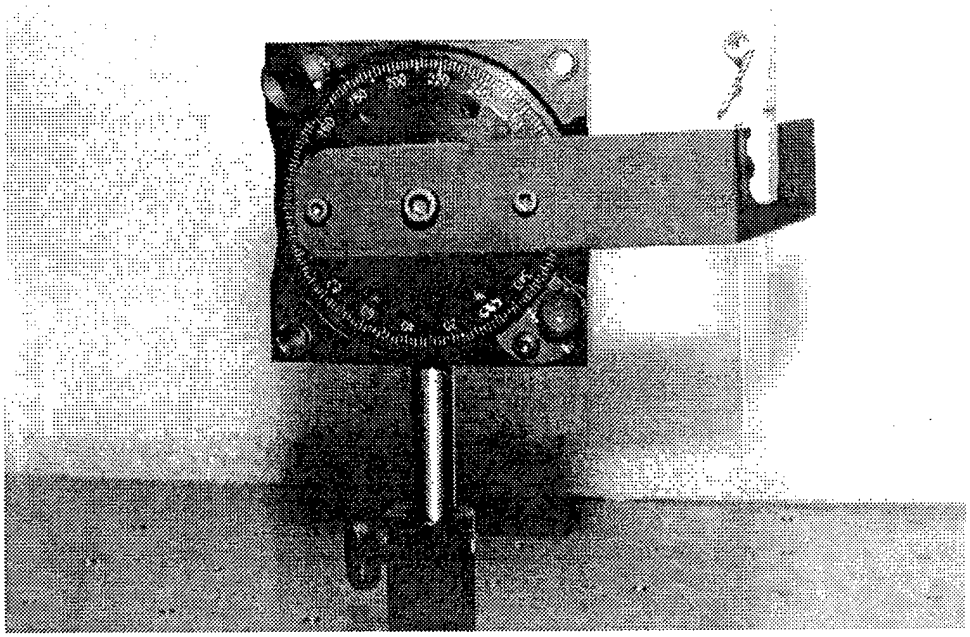

Figure 21. Microscope Slide Reflector.

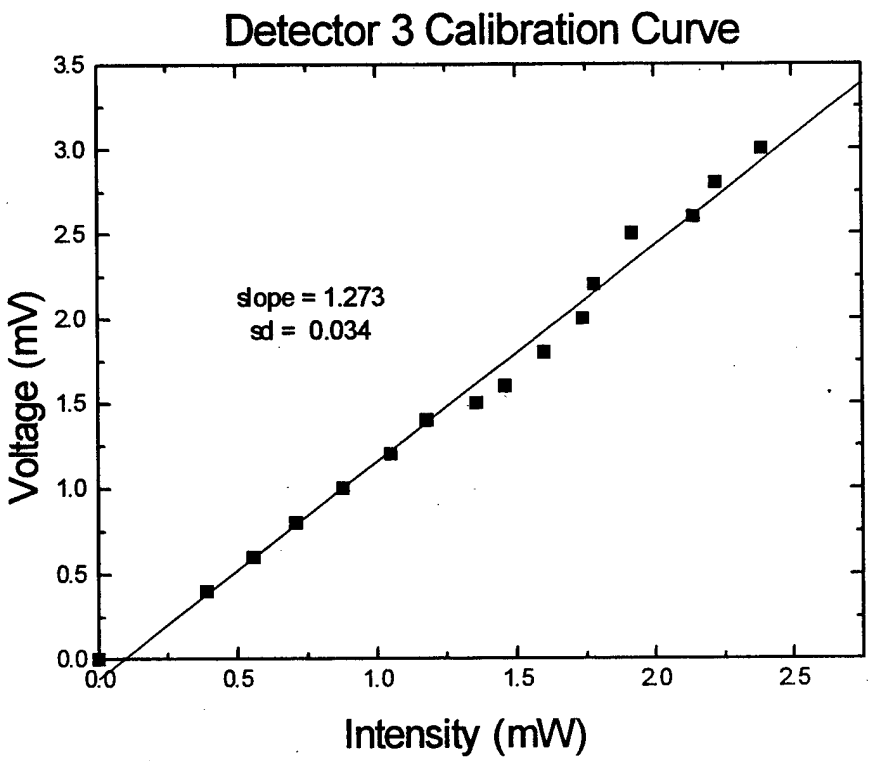

Figure 22. Detector 3 Calibration Curve.

The linearity of Detector 3 was checked by measuring its output voltage for different values of optical power incident on its window. The results are plotted in Figure 22.

Once DC alignment was complete, RF voltage was applied. The modulator was allowed to come to a steady state to take into account any crystal expansion due to heating from the oscillating voltage. Any slight crystal expansion increases the optical pathlength and thus also the phase difference Γ. The DC bias voltage was then adjusted to regain equal power readings on Detectors 1 and 2 to compensate for this thermal drift.

At frequencies above 20 MHz, radiation from the amplifier was being picked up by the oscilloscope probe. Thus it became necessary to provide RF shields (e.g., Faraday cages) for all instruments and connecting cables. A copper ground plate was installed beneath the circuit board which itself was mounted inside a cast aluminum box, and grounded to it. The aluminum housing of the modulator was grounded to the optics bench as well as the circuit box. Double shielded coaxial connectors used for all power or detector connections were again shielded inside copper braid. A large copper ground plate was placed underneath the instruments.

It was intended that RF voltage would be applied to the modulator at voltage steps of 40 V_{pp} from 40 V_{pp} to 160 V_{pp} at each frequency step. This is because 160 V_{pp} approximates the full transmission response range of the modulator. It was experimentally determined that the full voltage range was not attainable at frequencies greater than 20 MHz with the availiable RF amplifier, as discussed earlier in this chapter.

4. Results

The applied modulator voltage and the Detector 3 output were measured on the two channels of a Tektronix oscilloscope, Model 2445B with a bandwidth of 150 MHz for

frequencies up to 30 MHz, and Model 2465 with a bandwidth of 300 MHz for higher frequencies. The modulator voltage was measured with a x10 probe which was connected via 3 inch twisted leads through a hole in the side of the aluminum box. This precaution was taken so that the cover could be securely fastened to reduce RF pickup. This setup may be seen in the equipment photograph in Figure 10 of Chapter II. The microscope slide aligner was then adjusted to ensure that detector diode current read 100 μA on the detector power supply before any detector output oscilloscope readings were taken. The results are recorded below in Table 3. Note that the full 160 volt RF modulation voltage could not be attained above 15.7 MHz with this method, indicating that the Q-factor of the modulator was less than that of a commercial 82 pF capacitor. Modulation Percentage is calculated by half the peak-to-peak voltage divided by mean voltage of the detector output. A more complete data listing is provided in Appendix B.

V_{pp} at modulator input	Modulation Percentage at Frequency step				
	10.4 MHz	15.7 MHz	21.1 MHz	27.8 MHz	30.0 MHz
40	39.75	39.85	45.4	44.4	44.1
80	73.4	73.85	79.85	73.3	*
120	94.6	93.25	93.75	*	*
160	100	100	*	*	*

Table 3. Results obtained with transformer. Resonant frequencies are 10.4, 15.7, 21.1, 27.8, and 30.0 MHz. Values in table are arithmetic mean of data collected which is provided in Appendix B. Asterisks are data points which we were not able to obtain due to power amplifier output limit.

C. PARALLEL TUNED CIRCUIT

1. Introduction

For frequencies above 20 MHz, the transformer was replaced by a parallel tuned circuit as shown in Figure 23. The resonant frequency was varied through proper selection of

the inductor with or without a parallel capacitor. The equipment setup, with appropriate RF screening methods, remained the same as that used for lower frequencies which made use of a transformer. The 0.0050 μF capacitor provides an AC ground while allowing the use of the DC bias. The 100 kΩ resistor is present again to protect the DC power supply from an

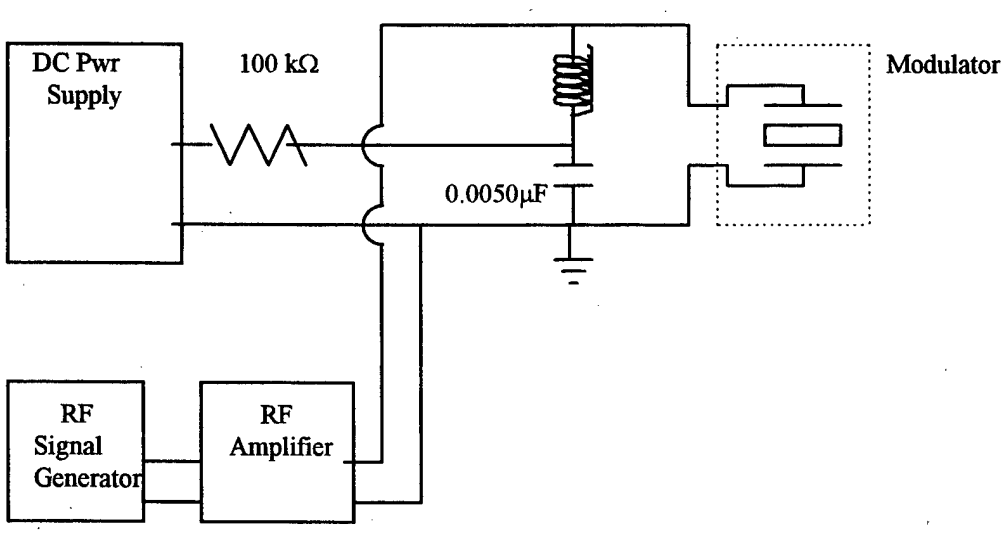

Figure 23. Parallel Tuned Circuit.

accidental short circuit. The RF amplifier with a maximum power output of 4 W (into a 50 Ω load) could not supply a voltage greater than about 50 V_{pp} to the parallel tuned circuit.

2. Experimental Procedure

As before, the DC bias was adjusted to ensure that the modulator operated at the 50 % transmission point. Once the resonant frequency was found, the RF applied voltage was set to 40 V_{pp}. The probe was connected exactly the same as before, when a transformer was used. The modulator was allowed to reach steady state and the DC voltage was then adjusted to compensate for any thermal drift. The slide aligner was adjusted to set the Detector 3 diode

current reading to 100 μA for each reading. The percentage modulation was determined as before.

3. Results

The results obtained are shown in Table 4.

It will be noticed that there is a considerable increase in the modulation percentage in the frequency range of 30-40 MHz with a significant maximum at 35 MHz, suggestive of some kind of resonance, either electrical in the circuit, or mechanical in the crystal. The

Frequency (MHz)	Optical Modulation
18.8	41.8
25.0	49.3
30.0	57.0
32.0	71.7
34.0	87.4
35.0	89.8
37.5	80.5
50.0	39.1
54.0	41.2
58.4	42.3
58.6	37.9
61.6	26.4
65.0	20.5
70.2	15.0
75.8	6.7
80.0	0
100.0	0
127.0	0

Table 4. Results for tuned circuit modulation. Values in table are arithmetic mean of data collected which is provided in Appendix B.

results are drastically different from the manufacturer's specifications. At first, it was thought that the inductance of the internal wire leads of the modulator formed a series resonance circuit with the modulator crystal capacitance of 82 pF, thereby producing a greater voltage

across the crystal than at the input terminals. To test this hypothesis, the impedance across the wire leads to the modulator was measured as a function of frequency using the HP 4194A Impedance / Gain-Phase Analyzer, in the frequency range from 10 MHz up to the frequency limit of the analyzer (40 MHz). The modulator was connected to the analyzer with 2 1/2 inch straight leads and with 2 1/2 inch twisted leads. The impedance of an 82 pF capacitor was also

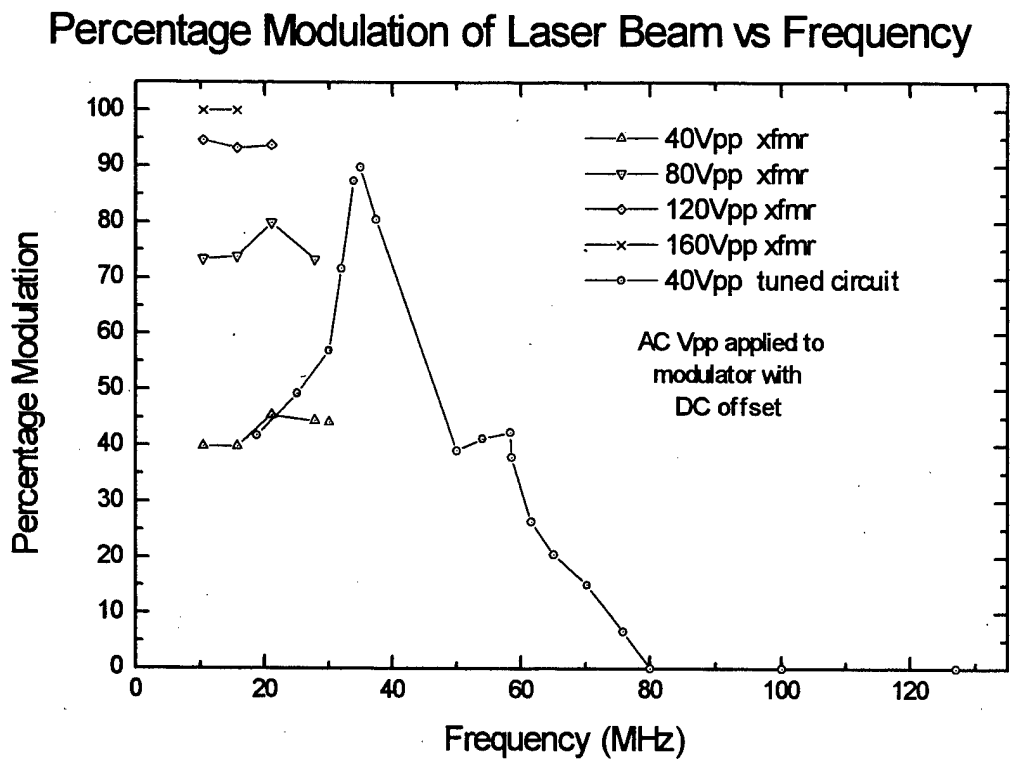

Figure 24. Modulation Percentage vs. Frequency. Results are plotted for both transformer and parallel tuned circuit modulation methods.

(a)

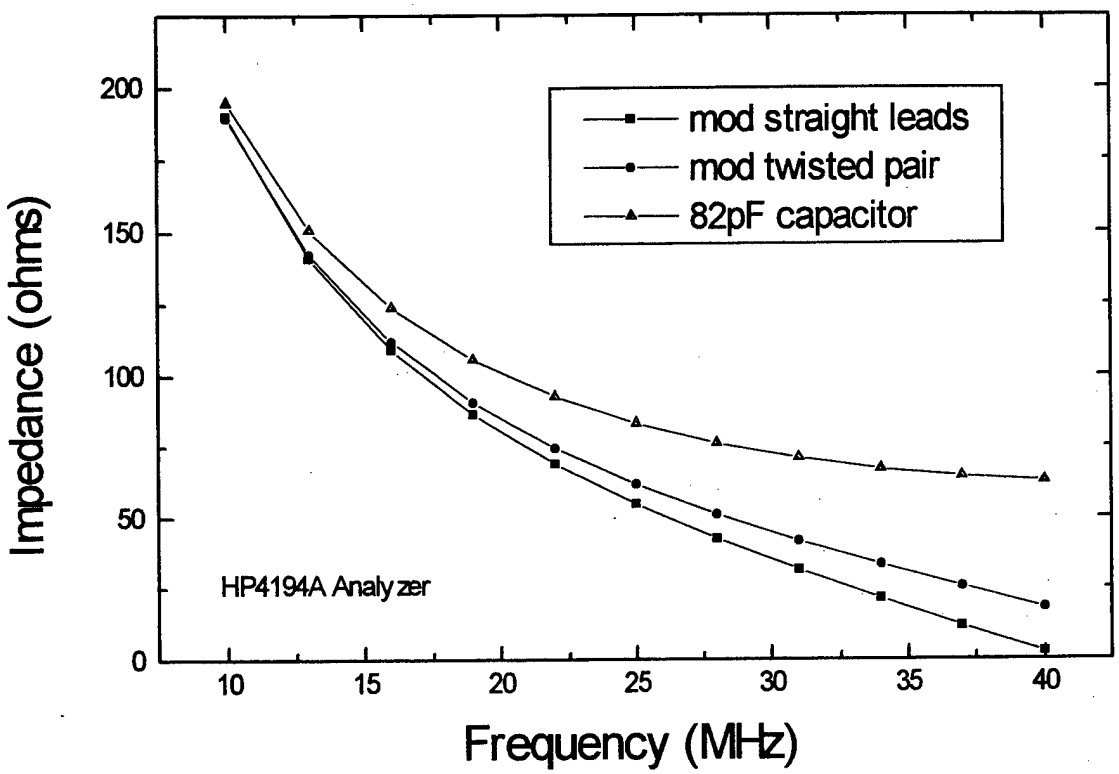

(b) (c)

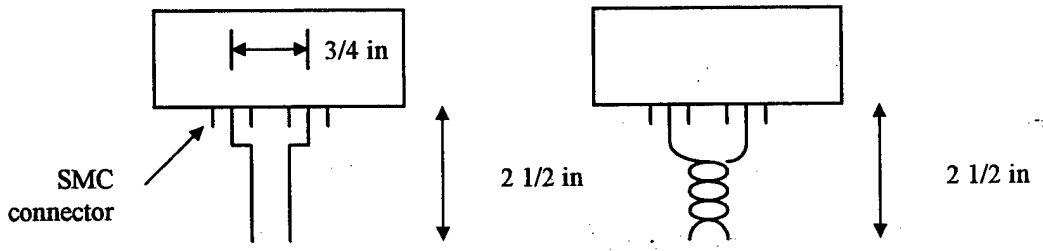

Figure 25. Modulator Response. Measurements (a) were done with 2.5 inch straight leads (b) and 2.5 inch twisted leads (c) from the modulator to the HP4194A analyzer. An 82 pF capacitor is shown for comparison.

measured in the same frequency range, for comparison with the modulator data. The results, shown in Figure 25, clearly demonstrate the presence of an inductive reactance. This inductance would seem to be the reason for the natural resonance of 35 MHz. This would also provide the reason for the decrease in response at higher frequencies. At higher frequencies, the reactance of the inductance would drastically reduce the voltage applied to the modulator crystal.

The unexpected behavior of the modulator was brought to the attention of the manufacturer's technical staff in Germany on 13 May. They reiterated their previous claim that their laboratory measurements yielded a flat frequency response with a 3 dB drop at 100 MHz. They attributed the peak in the frequency response to the external electrical circuit.

Further tests on the circuit revealed that the voltage measured with the x10 probe applied directly to the modulator terminals, at 35 MHz, was nearly 2 1/2 times the voltage at the input to the twisted leads. At frequencies above 60 MHz, the voltage measured at the modulator decreased considerably. This confirmed the existence of an inductive reactance between the input to the twisted leads and the modulator crystal capacitance.

It will be recalled that the driver circuit (Figure 23) was designed to enable the insertion of different inductors to resonate with the capacitance (82 pF) of the modulator at discrete frequencies between 20 MHz and 150 MHz, in a parallel RLC circuit. The objective of this arrangement was to ensure that the impedance presented by the driver circuit to the output of the RF amplifier was purely resistive, or nearly so. This arrangement worked satisfactorily when the circuit was tested with a ceramic disk capacitor located in close proximity to the inductor. However, the measurements described in the previous paragraphs show that the arrangement failed to give satisfactory results when used with the modulator,

owing to the presence of unavoidable inductive loops, both external and internal, in the connections from the inductor to the crystal capacitor within the modulator.

Guided by a block diagram supplied by the manufacturer's technical staff, it was decided to drive the modulator through a coaxial cable connected to one of the SMC connectors on the modulator, with the other SMC connector grounded. This arrangement precluded the use of an inductor to resonate with the crystal capacitor. Nor did it make it possible to measure and regulate the RF voltage at the modulator terminals so as to determine the true frequency response of the modulator. But it did eliminate the inductive loop in the external open connections to the modulator.

The DC and RF voltages were both supplied through the same coaxial cable with the help of a hybrid circuit. The arrangement is shown in Figure 26. The internal electrical circuit of the modulator, composed of the capacitance of the crystal in series with the inductance of the internal wire leads to the electrodes, together with the coaxial cable, present a complicated load impedance to the output of the amplifier, making it impossible to take advantage of the amplifier's maximum rated output of 4 W (into a 50 Ω resistive load). Furthermore, the input voltage to the amplifier was limited to the value specified by its manufacturer to avoid the damage that would result from the gross mismatch between the output impedance and the load impedance, at high power levels. Taking these precautions, it was found by trial and error that the best performance attainable was an amplitude modulation of the laser beam intensity of about 25 percent at a frequency of 125 MHz.

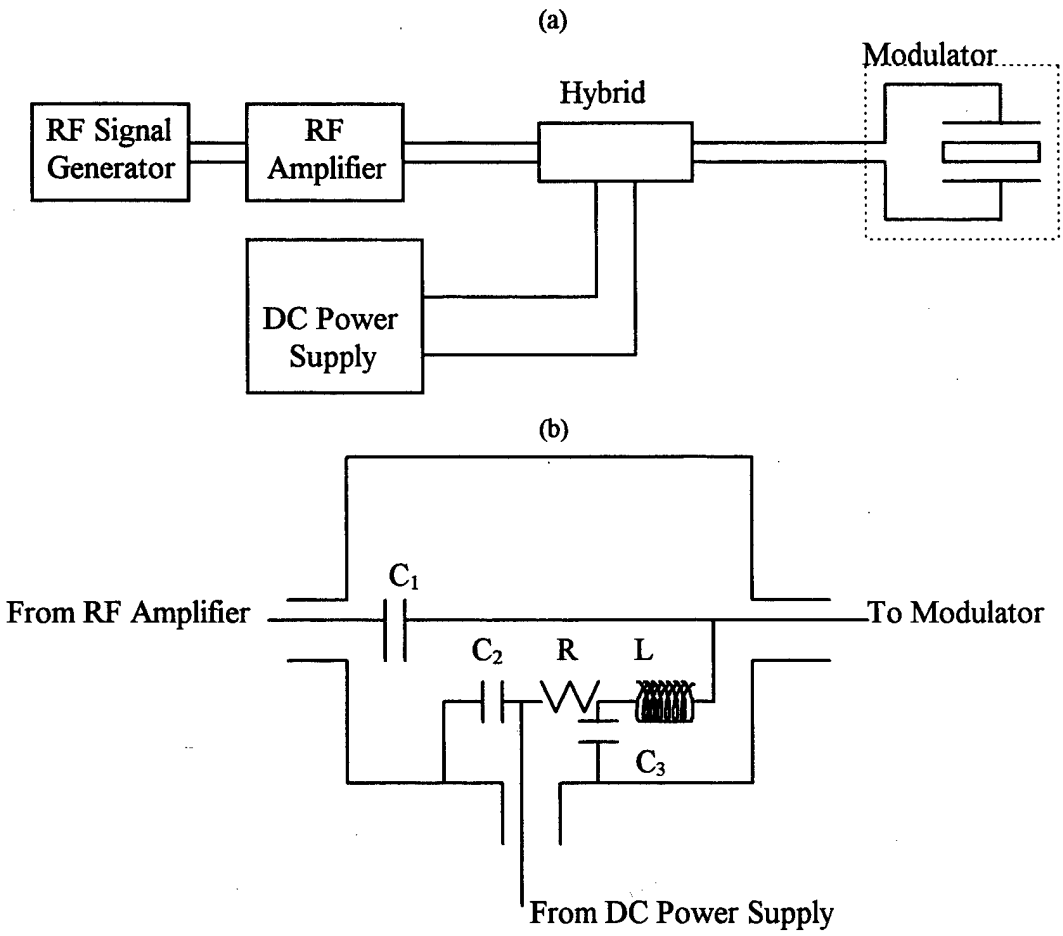

Figure 26. Setup. (a) Equipment set up with no RF voltage monitoring. *Connections between components are via coaxial cable.* (b) Close Up of Hybrid Connector. C_1 = 0.01 μF 500V, C_2 and C_3 = 0.0047 μF 500 V, R = 100 kΩ 1/2 W, L = RF choke 1 μH.

IV. RESULTS AND CONCLUSIONS

A. ANALYSIS OF RESULTS

The real challenge of this thesis has been in determining the frequency response of the LM 0202 P modulator. Amplitude Modulation at the highest frequency possible and the highest percentage modulation was desired for use in proving the amplitude to frequency modulation conversion in fiber optic cables. To find the highest possible frequency, the characteristics of the LM 0202 P modulator had to be determined with the aid of relatively inexpensive driving circuits. To measure the frequency response properly, a radio frequency voltage of known constant amplitude must be applied to the modulator, over the desired frequency range, and the amplitude modulation of the laser beam must be properly measured. Several circuits were developed and tested for this purpose, but none of them worked satisfactorily at frequencies above 30 MHz. It proved to be impossible to achieve any perceptible modulation above 80 MHz.

An analysis of the problem indicated that any circuit which made provision for the accurate measurement of the RF voltage across the modulator terminals (the center pins of SMC connectors), which were separated by 3/4 inch, would introduce an inductive loop into the circuit, and the loop could have a sufficiently high impedance at high frequencies to prevent the RF voltage from reaching the modulator crystal. The real problem was the large separation between the modulator terminals. At the commencement of the measurements, it was not thought that this separation would cause problems, because the manufacturer had claimed that the 3 dB bandwidth of the modulator was greater than 100 MHz. In the light of the measurements made for this thesis, it seems clear that the

manufacturer should have fitted to the modulator a single SMC, or BNC, coaxial bulkhead connector to provide electrical connection to the crystal inside the modulator. This would have minimized the size of any inductive loop, internal or external.

The shortcoming in the construction of the modulator was brought to the notice of the manufacturer in Germany. It was then discovered, belatedly, that the experimental arrangement used by them did not make provision for the measurement of the RF voltage across the modulator terminals. They had not determined the frequency response of the modulator by maintaining the RF input voltage constant and measuring the frequency at which the percentage modulation of the laser beam dropped to 3 dB below the value at low frequency, as they should have done. Instead, they had used a servo system to correct for any change in the percentage modulation, as the frequency was increased, by automatically varying the input RF voltage. The 3 dB point, which they found to be about 100 MHz, was not the result of a limitation in the crystal circuit, but a consequence of the maximum power output of the RF amplifier used by them.

B. CONCLUSIONS AND RECOMMENDATIONS

It has not been practicable to realize one of the objectives of this investigation, which was to determine the frequency response of the LM 0202 P electro-optic modulator by measuring the percentage amplitude modulation of the laser beam as a function of frequency, with the input RF voltage maintained constant. However, the use of an experimental arrangement which dispensed with the measurement of the applied RF voltage (described in C of Chapter III) has made it possible to achieve amplitude modulation of the laser beam at a frequency as high as 125 MHz, with a percentage

modulation of twenty-five percent. This performance is superior to that claimed by the manufacturer.

Amplitude modulation at any specific frequency can only be obtained with an RF amplifier designed from the start with enough power at the desired frequency and capable of providing 160 V_{pp} RF to the modulator. Future thesis research aimed at proving the amplitude to frequency modulation in fiber optic cables using the LM 0202 P electro-optic modulator should be directed along this line of experimentation. If modulation at higher frequencies than 150 MHz is desired, alternate methods of modulation, such as optical switching, must be considered.

APPENDIX A LASER SPECIFICATIONS AND OPERATING PROCEDURES

1. Manufacturer's Laser Characteristics

Manufacturer	Lexel
Model	Model 85 Series
Serial Number	4706H
Class	3b
Type	Argon Ion
Mode	CW
Wavelength	0.488 - 0.514 μm
Max Power	300 mW for 514.5 nm wavelength
Beam Diameter	1.1 mm (at 1/e points)
Beam Divergence	0.7 mrad
Beam Polarization ratio	>100:1 E vector vertical
Cavity Length	0.80 m
Amplitude power stability	<±0.2% in light control

2. Hazard Evaluation

Maximum Permissible Exposure	$2.5E^{-3}$ W / cm^2
Nominal Ocular Hazard Distance	246.9 m
Minimum Optic Density for Eyewear	5 @ λ 0.488 - 0.514 μm
Maximum Permissible Exposure	3.1 W / cm^2
Hazard Distance Skin	6.9 m
Maximum Permissible Exposure	$6.5E^{-3}$ W / cm^2
Safe Viewer Distance From Diffuse Reflection	20 cm

$E_o = 62.6$ W / cm^2

3. Routine Operation (from [8])

After the laser has been operated initially, it may be routinely started in either the current- or light-control mode by following these steps:

1. Check to be sure the LINE and FUSE indicators are lighted.

2. Turn the key in the KEY CONTROL to the "ON" position.

3. Turn on the cooling water, and check to see that the INTLK indicator is lighted.

4. Press the POWER ON switch. The POWER indicator and the LASER RADIATION EMISSION indicators will light.

5. After the READY indicator has lighted, press the LASER START switch (unless using the automatic starting option.)

6. Adjust the appropriate CURRENT CONTROL or LIGHT CONTROL knob to set the operating level.

Current Control

When the laser is operated in the current-control mode, the plasma-tube current is maintained at a preselected level. This mode of operation provides a reasonable constant optical power output, but it does not compensate for any minor changes in the positions of the optical components over time, which can result in slight variations in the output power. In the current-control mode, maximum stability will be attained after approximately 30 minutes of operation.

By turning the CURRENT CONTROL knob, the plasma-tube current may be adjusted from the approximately six amperes to a maximum value that has been preset at the factory. No attempt should be made to alter this upper limit.

The operating level of the current can be read on the LASER meter on the front panel of the power supply when the selector switch is in the "CURRENT 25A" position.

When the plasma-tube current is adjusted to a very low level, the tube may sometimes deionize and go out. If this should happen, turn the CURRENT CONTROL knob clockwise to a higher current setting before attempting to restart the laser. If the current is left at a very low setting, the laser may not start.

If the laser is equipped with a Model 7501 Light Regulator, always remember to turn the laser for peak power output in the current-control mode of operation. Since the

plasma-tube current will be held constant, this ensures that any changes in the optical output power will be due to mirror tuning alone.

Light Control (Option 7501)

When the laser is operated in the light-control mode, a small portion of the laser's light output is sampled by a beamsplitter in the light sampler assembly inside the front of the laser head. This sampled light is detected by a silicon photocell, and an electrical voltage proportional to the intensity of the light is fed back to the regulator circuitry. A differential amplifier in the regulator compares this signal voltage with a reference voltage level that is set by the LIGHT CONTROL potentiometer on the front panel of the power supply; it then generates an error signal proportional to the difference between the two. The error signal is amplified to drive the power transistors in the regulator passbank, causing them to increase or decrease the plasma-tube current as required to maintain the output beam at a constant optical power level. In fact the plasma-tube current may vary considerably.

Since the current has a factory-set upper limit, it is advisable to allow a margin of several amperes between this limit and the current required to obtain a desired power output. If the laser is operated at the maximum possible current in light-control, it can drift out of regulation due to temperature-caused mirror detuning or other minor physical changes.

If the BEAM ATTENUATOR is placed in the "CLOSED" position while the laser is operating in light-control, the plasma-tube current will rise to the maximum current limit. While this is no more damaging to the laser than normal high-current operation,

permitting the unit to "idle" at this high current level for extended periods of time serves no useful purpose and will have an eventual effect on the life of the plasma tube.

To operate in light control:

1. Switch the CONTROL SELECTOR to the "LIGHT" position.
2. If the unit is equipped with a panel-mounted power meter (option 7507), it is merely necessary to set the selector switch to the power range desired, then adjust the LIGHT CONTROL knob to obtain a specific output power, as indicated on the LASER POWER meter.
3. If the unit is not equipped with a panel-mounted power meter, it will be necessary to use a separate laser power meter to measure the intensity of the output beam. With the external power meter turned on and intercepting the beam, set the LIGHT RANGE switch to the appropriate position, then adjust the LIGHT CONTROL knob to obtain the exact power level desired.

APPENDIX B DATA

1. **Detector 1 and 2 Data**
2. **Applied DC Voltage to Optical Modulator**
3. **Linearity of Modulator Internal Circuit**
4. **Linearity of Modulator Optical Response to Applied AC Voltage**
5. **Detector 3 Calibration Data**
6. **Tektronix 2445B Oscilloscope Probe Calibration**
7. **Tektronix 2465 Oscilloscope Probe Calibration**
8. **Modulation Data (Circuit using transformer)**
9. **Modulation Data (Parallel Tuned Circuit)**
10. **Modulator Impedance Data**

1. Detector 1 and 2 Data

mW	mV DET 1	mV DET 2
6.7	65	70
10.0	100	100
15.0	145	150
20.0	200	200
25.0	250	250
30.0	300	300
35.0	350	345
40.0	395	400
45.0	450	445
50.0	500	495

Table B1. Detector 1 and 2 Response Data.

This data was taken by placing the detectors in the path of the laser output from the Argon-Ion laser. The output power was controlled at the laser power supply and varied in light control. Column 1 is the reading on the digital meter in the Newport Model 815 Series Power. Column 2 and 3 are read from a Tektronix 2445B oscilloscope coming from the analog outputs on the back of the detector power supplies.

2. Applied DC Voltage to Optical Modulator

Applied DC Voltage to Modulator					
Floating			Grounded		
V DC	DET 1	DET 2	V DC	DET 1	DET 2
0	32.0	32.3	0	32.8	31.7
10	26.2	37.5	10	26.7	37.2
20	20.3	42.7	20	20.7	42.6
30	14.8	47.5	30	15.3	47.4
40	10.1	51.8	40	10.5	51.8
50	6.2	55.3	50	6.6	55.4
60	3.3	57.9	60	3.5	58.3
70	1.4	59.7	70	1.5	60.1
80	0.6	60.4	80	0.7	60.9
90	1.0	60.1	90	1.0	60.7
100	2.4	58.8	100	2.4	59.5
110	5.0	56.5	110	4.9	57.2
120	8.5	53.3	120	8.4	54.0
130	13.0	49.4	130	12.8	50.1
140	18.1	44.8	140	17.9	45.5
150	23.9	39.7	150	23.7	40.3
160	29.9	34.4	160	29.9	34.9
170	36.2	28.8	170	36.2	29.3
180	42.4	23.3	180	42.5	23.8
190	48.2	18.1	190	48.6	18.5
200	54.0	13.0	200	53.9	13.6
210	58.4	9.1	210	58.8	9.2
220	62.3	5.6	220	62.7	5.8
230	65.4	2.8	230	65.9	3.1
240	67.5	1.1	240	68.1	1.2
250	68.5	0.3	250	69.2	0.4
260	68.4	0.5	260	69.0	0.6
270	67.0	1.8	270	67.6	1.8
280	64.5	4.0	280	65.1	4.0
290	60.9	7.0	290	61.7	7.1
300	56.4	11.0	300	57.2	11.0

Table B2. Data for Applied DC Voltage to Optical Modulator.

Both sets of data taken to check to see if grounding output lead to modulator changed output of modulator. Grounded DC voltage and output power data plotted.

3. Linearity of Modulator Internal Circuit

Modulator Linearity		
V_{pp} primary	Applied V_{pp}	mV_{Rpp}
0.5	13	110
1.0	27	250
1.5	41	375
2.0	55	510
2.5	69	645
3.0	84	783
3.5	99	910
4.0	113	1052
4.5	130	1205
5.0	143	1320
5.5	160	1480
6.0	175	1615

Table B3. Modulator Linearity Measurements.

4. Linearity of Modulator Optical Response to Applied AC Voltage

Linearity of Optical Response		
Applied V_{pp} to primary	Applied V_{pp} across secondary	DET 3 mV_{Rpp}
0.5	17	0.93
1.0	33	1.60
1.5	50	2.61
2.0	66	3.37
2.5	83	3.88
3.0	98	4.55
3.5	116	4.97
4.0	130	5.39
4.5	149	5.56
5.0	162	5.80

Table B4. Linear Response of Modulator Data.

Detector 3 Output read from Tektronix 2445B Oscilloscope.

5. Detector 3 Calibration Data

o-scope reading (mV)	DET 3 (mW)*
0.0	0
0.4	0.39
0.6	0.56
0.8	0.71
1.0	0.88
1.2	1.05
1.4	1.18
1.5	1.36
1.6	1.46
1.8	1.60
2.0	1.74
2.2	1.78
2.5	1.92
2.6	2.14
2.8	2.22
3.0	2.39

Table B5. Detector 3 Calibration Data.

This data was taken by placing the Detector 3 in the path of the laser beam reflected from the microscope slide. The output power is controlled at the laser power supply and varied in light control. Column 1 is the output of Detector 3 read from a Tektronix 2445B oscilloscope. Column 2 is the laser power incident on Detector 3 using Detector 1 and the Newport Model 815 Power Meter in its place.

6. Tektronix 2445B Oscilloscope Probe Calibration Process

Tektronix 2445 B 150 MHz Oscilloscope with TEK 6133 10x probe
- used for transformer action circuit

The calibration of the oscilloscope was first checked with a 1x probe connected from the function generator to the oscilloscope at the 50 Ω input setting, and found to be accurate.

The input setting was changed to the 1 MΩ setting with the following results:

frequency (MHz)	AC V_p	O-scope V_{pp}
1	10	20.2
10	10	20.6
20	10	22.0
30	10	20.8

(a)

The 1x probe was changed to the 6133 x10 probe with the following results:

frequency (MHz)	AC V_p	O-scope V_{pp}
1	10	20.4
10	10	20.3
20	10	23.4
30	10	22.4

(b)

After calibration of the x10 probe:

frequency (MHz)	AC V_p	O-scope V_{pp}
1	10	20.0
10	10	20.0
20	10	20.4
30	10	21.8

(c)

Table B6 (a-c). Calibration Data for oscilloscope probe.

7. Tektronix 2465 Oscilloscope Probe Calibration

Tektronix 2465 300 MHz Oscilloscope with TEK 6134C 10x probe
- used for parallel tuned circuit measurements

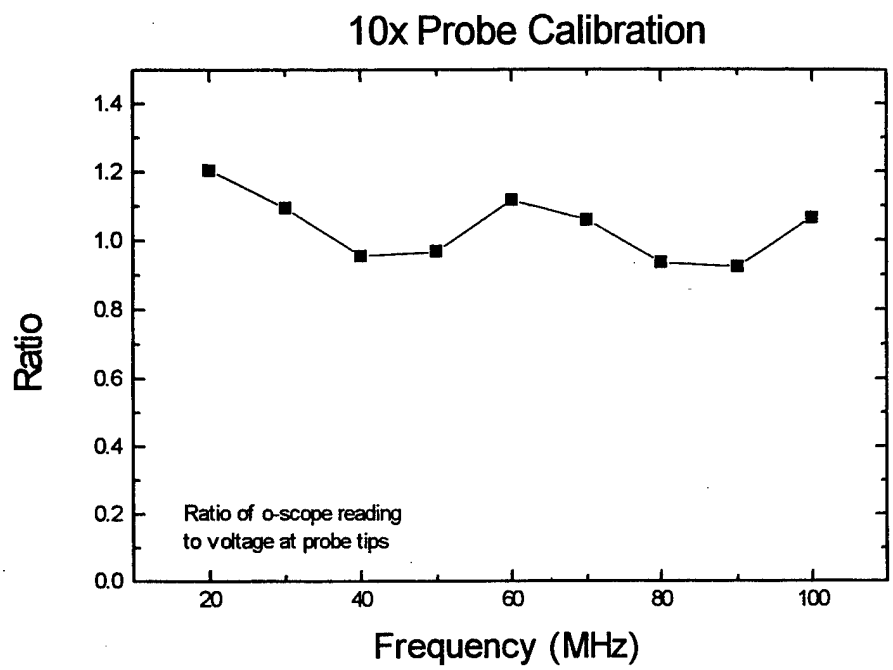

Figure B1. x10 Probe Calibration Data.

Frequency (MHz)	Correction factor	Signal Generator Vpp Reading	Corrected Vpp reading at probe tips	O-scope reading Vpp	Ratio
20	0.997	7.07	7.054	8.5	1.204
30	0.995	7.07	7.035	7.7	1.094
40	0.991	7.07	7.009	6.7	0.955
50	0.986	7.07	6.975	6.75	0.967
60	0.980	7.07	6.935	7.75	1.117
70	0.974	7.07	6.888	7.3	1.059
80	0.966	7.07	6.835	6.4	0.936
90	0.958	7.07	6.777	6.25	0.922
100	0.949	7.07	6.713	7.15	1.064

Table B7. Tektronix 6134C Calibration Data.

$$\text{Correction factor} = \left| \frac{-j/\omega c}{R - j/\omega c} \right| = \frac{1}{\sqrt{1+(R\omega c)^2}}$$

8. Modulation Data (Circuit using transformer)

AC Vp	AC function generator peak-to-peak output voltage applied to the input of the amplifier, which is connected to primary of transformer
Applied Vpp	Applied AC peak to peak voltage to modulator from secondary of transformer
V1, V2	minimum/maximum voltages of Detector 3 output

A $(V2 - V1)/2$ amplitude of sinusoidal voltage

B $(V2 + V1)/2$ mean voltage

modulation percent = A/B

AC V_p	Applied V_{pp}	V1	V2	A	B	Optical Percent
0.0235	40	3.15	7.25	2.05	5.20	39.4
		3.10	7.25	2.08	5.18	40.1
0.0467	80	1.30	8.45	3.58	4.88	73.3
		1.30	8.50	3.60	4.90	73.5
0.0707	120	0.25	9.90	4.83	5.08	95.1
		0.30	9.85	4.78	5.08	94.1
0.0937	160	0	10.30	5.15	5.15	100
		0	10.25	5.13	5.13	100

Table B8. 10.44 MHz Data.

At 160 Vpp, the peaks of the output are slightly flattened. The transformer used has a 40 turn, 1/2 inch diameter, 14 gauge enameled copper wire secondary with a 4 turn primary coil. Primary capacitor was 330 pF.

AC V_p	Applied V_{pp}	V1	V2	A	B	Optical Percent
0.0377	40	3.05	7.20	2.08	5.13	40.5
		3.10	7.10	2.00	5.10	39.2
0.0757	80	1.35	9.10	3.88	5.23	74.2
		1.40	9.15	3.88	5.28	73.5
0.117	120	0.40	10.75	5.18	5.58	92.8
		0.35	10.75	5.20	5.55	93.7
0.168	160	0	10.25	5.13	5.13	100
		0	10.20	5.10	5.10	100

Table B9. 15.70 MHz Data.

At 160 Vpp, the peaks of the output are slightly convex. The transformer used has a 20 turn, 1/2 inch diameter secondary coil with a 2 turn primary coil. Primary capacitor was 100 pF.

AC V_p	Applied V_{pp}	V1	V2	A	B	Optical Percent
0.059	40	3.05	8.05	2.50	5.55	45.1
		3.00	8.05	2.53	5.23	45.7
0.118	80	1.10	10.00	4.45	5.55	80.2
		1.15	10.10	4.48	5.63	79.5
0.195	120	0.35	10.90	5.28	5.63	93.7
		0.35	10.80	5.23	5.58	93.8

Table B10. 21.06 MHz Data.

The transformer used has a 10 turn, 1/2 inch diameter secondary coil and a 2 turn primary coil. Primary capacitor was 68 pF.

AC V_p	Applied V_{pp}	V1	V2	A	B	Optical Percent
0.074	40	3.05	8.00	2.48	5.53	44.8
		3.10	7.95	2.43	5.53	43.9
0.150	80	1.4	9.5	4.05	5.45	74.3
		1.5	9.65	4.08	5.65	72.2

Table B11. 27.8 MHz Data.

Transformer has a 10 turn, 1/4 inch diameter secondary coil with a 2 turn primary coil. Resistor in primary was 20 Ω and the primary capacitor was 330 pF.

AC V_p	Applied V_{pp}	V1	V2	A	B	Optical Percent
0.088	40	3.20	8.15	2.48	5.68	43.6
		3.15	8.20	2.53	5.68	44.5

Table B12. 29.98 MHz Data.

Transformer has a 10 turn, 1/8 inch diameter secondary coil with a 2 turn primary coil. Primary capacitor was 220 pF.

9. Modulation Data (Parallel Tuned Circuit)

Frequency (MHz)	Applied V_{pp}	V1	V2	A	B	Optical Percent
18.8	40	1.55	3.70	1.10	2.63	41.8
		1.45	3.55	1.05	2.50	42.0
25	40	1.35	4.00	1.33	2.68	49.4
		1.40	4.10	1.35	2.75	49.1
30	40	1.20	4.50	1.65	2.85	57.9
		1.25	4.45	1.60	2.85	56.1
32	40	0.70	4.40	1.85	2.55	72.5
		0.75	4.40	1.83	2.58	70.9
34	40	0.35	4.75	2.20	2.55	86.3
		0.30	4.85	2.28	2.58	88.4
35	40	0.30	5.60	2.65	2.95	89.8
		0.30	5.60	2.65	2.95	89.8
37.5	40	0.40	4.20	1.90	2.30	82.6
		0.50	4.10	1.80	2.30	78.3
50	40	1.65	3.85	1.10	2.75	40.0
		1.70	3.80	1.05	2.75	38.2
		1.80	4.10	1.15	2.95	39.0
54	40	1.55	3.80	1.13	2.68	42.2
		1.60	3.75	1.08	2.68	40.2
58.4	40	1.50	3.70	1.10	2.60	42.3
		1.55	3.80	1.13	2.68	42.2
58.56	40	1.55	3.40	0.93	2.48	37.5
		1.50	3.35	0.93	2.43	38.3
61.6	40	1.90	3.30	0.70	2.60	26.9
		2.00	3.40	0.70	2.70	25.9
65	40	2.20	3.30	0.55	2.75	20.0
		2.20	3.35	0.58	2.78	20.9
70.16	40	2.30	3.10	0.40	2.70	14.8
		2.25	3.05	0.40	2.65	15.1
75.8	40	2.65	3.05	0.20	2.85	7.0
		2.65	3.00	0.18	2.83	6.4
80	40	*	*	*	*	0
100	40	*	*	*	*	0
127	40	*	*	*	*	0

Table B13. Parallel Tuned Circuit Data.

Asterisk values indicate readings which could not be measured with the Tektronix 2465 Oscilloscope at its highest sensitivity.

10. Modulator Impedance Data

Frequency (MHz)	Impedance (Ω) mod straight leads	mod twisted leads	82 pF capacitor
10	190.0	189.4	194.7
13	141.1	142.3	150.9
16	109.3	112.1	123.9
19	86.6	90.8	105.8
22	69.1	74.7	92.9
25	54.8	61.8	83.4
28	42.5	51.1	76.3
31	31.6	41.8	71.0
34	21.4	33.4	67.1
37	11.6	25.6	64.4
40	2.7	18.1	62.9

Table B14. Modulator Impedance Data taken with HP4194A Analyzer.

APPENDIX C. EQUIPMENT SPECIFICATIONS

1. **Optical Modulator LM 0202 P**
2. **Transformer (used for measurements at 1 kHz)**
3. **Model 815 Digital Power Meter and Photosensor**
4. **Series PD30-03 Ultra High Speed Photodetector**
5. **Five Axis Alignment Platform**
6. **Mini-Circuits RF Power Amplifier**

1. Optical Modulator LM 0202 P Characteristics

Manufacturer	Gsanger Optoelektronik GmbH
model	LM 0202 P 5 W
Description	Intensity modulator
Spectral Range	250 - 1100 nm
Aperture	3 x 3 mm
Power Capability	0.1 - 5 W
Extinction	1:250
Transmission	95 %
Half - wave voltage	160 V (at 488 nm)
Wedge	0
Wavefront distortion	$\lambda/4$
Dimensions	Φ50 x 138 mm
Comments	4 crystals ADP or KD*P in order of compensation

Manufacturer's Operating Principles and Instructions

1. Introduction

Electro optic crystals change the optical pathlength upon application of an electric field. This change is polarization sensitive. The difference in pathlength of orthogonally polarized beams will be just one half of the wavelength, if the half wave voltage is applied. If the crystal is oriented suitably, the polarization direction of the transmitted light will be rotated by 90°. The light will be extinguished in this polarization state by a polarizer. Variation of the applied voltage allows quick modulation of the laser beam intensity. Performance of an electro optic modulator can be understood very simply as that of a retardation plate with electrically adjustable retardation.

Series LM 0202 laser modulators are using the transverse electro optic effect: the directions of the light beam and electric field are orthogonal. In this configuration long crystals with small width have a low half wave voltage.

Since most of the electro optic crystals operate with a strong background of natural birefringence, a compensation scheme is used: each modulator of the LM 0202

series contains 4 crystals as a matched ensemble. These crystals are fabricated with deviation from equal length smaller than 0.1 μm. These crystals are operated optically in series and electrically in parallel. Crystal orientation is such that for the intensity modulator (LM 0202 xx P) and the general purpose polarization modulator (LM 0202) retardation caused by natural birefringence is minimized. Just as in an ordinary retardation plate, the polarization of the laserbeam has to be adjusted to 45 ° to the optical axis in order to achieve proper 90 ° rotation.

If the laserbeam is polarized in the direction of the optical axis, no polarization rotation but pure phase retardation will occur. In principle this allows the user to operate every LM 0202 modulator as a phase modulator. Since in the configuration optimized for minimum background retardation only half of the crystals are electroptically active for phase modulation, a special phase modulator (LM 0202 PHAS) is available. This model has a different crystal configuration that does not remove the retardation background due to natural birefringence, but uses all 4 crystals for phase modulation effectively.

Due to the compensation scheme no beam displacement or deviation occurs in either case. A thick aluminum housing guarantees good thermal and mechanical stability.

2. Adjustment and Operation

Electro optic modulators require (generally linearly) polarized laser light. In case the laser is not sufficiently polarized by itself an additional polarizer has to be used.

The LM 0202 xx P model has an integrated polarizer that most commonly is used as an analyzer. The side of the modulator with the analyzer has to be put downstream. It can easily be recognized by the extra plate that is used as a polarizer mount.

In the first step the laser has to be aligned with the axis of the cylindrical modulator housing. This can be achieved by centering the beam on the modulator entrance face and subsequently tilting the modulator such that the back reflex is falling in the laser beam. The usable aperture of the modulator is 3 x 3 mm (for the standard version) exactly centered within the cylindrical housing.

In the second step the azimuthal rotation of the modulator has to be adjusted. The LM 0202 general purpose modulators and LM 0202 xx P intensity modulators require the direction of laser polarization to be at 45 ° to the edge of the crystals. These are defining the quadratic aperture and can be seen through the entrance window. These crystals are useful as reference for coarse adjustment.

Fine adjustment is best achieved operating the modulator between parallel polarizers. Keeping the laser polarization fixed, the optimum azimuthal rotation of the modulator is found by putting an offset voltage plus half wave voltage to the banana plugs. These plugs are isolated from the housing and directly connected to the crystals. A change of the laser intensity can be observed when the voltage between the banana plugs is varied. At minimum intensity a further decrease can be achieved by adjusting the azimuthal rotation of the modulator. By subsequently adjusting rotation and voltage, an extinction of better than 1 : 250 can be achieved.

Selected models with better extinction are available on request.

The modulator is tested for voltages up to 500 V. In case maximum extinction seems to require a higher voltage, reversing the polarity at the banana plugs will help.

Operating an electro optic modulator between crossed or parallel polarizers yields an intensity variation as given by:

$$I = I_o \sin^2 \left(U / U_{\lambda/2} \, \pi/2 \right)$$

where

$U_{\lambda/2}$	half wave voltage
I_o	input intensity
U	signal voltage.

It has been assumed that the appropriate offset voltage for maximum extinction is applied in addition.

In many cases it is advantageous to choose an offset voltage such that to first order the intensity varies linearly with voltage. This is achieved by setting the offset voltage to the value required for maximum extinction minus 1/2 U_2. A negative value can be realized by reversing polarity.

3. Maintenance

LM 0202 modulators are sealed hermetically. They can be operated at pressures from 100 to 1500 mB and at temperatures from 0 ° C to 50 ° C. Standard models are for horizontal use. Modulators for vertical use also are available on request. The cleaning of the windows can easily be achieved with an organic solvent.

2. Transformer (used for measurements at 1 kHz)

Manufacturer	Triad Transformer Corp, Los Angeles, CA
Data	GR 1 CL A FAM 01
	Triad No. 9782
	PK WKG V (5 -6) - 535 V

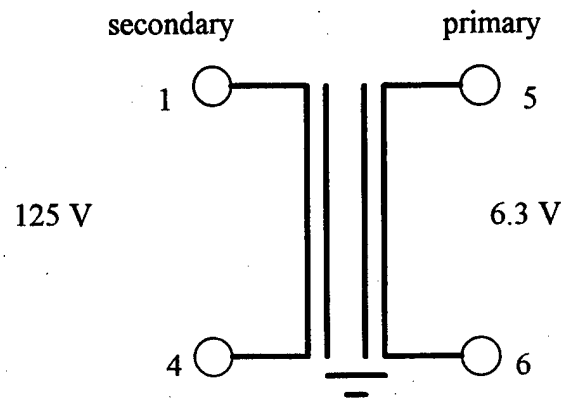

Figure C1. 1 kHz Transformer Diagram.

3. Model 815 Digital Power Meter and Photosensor

Manufacturer	Newport Corporation, Fountain Valley, California
Meter	
Ranges	.002, 0.02, 0.2, and 2 W with filter
Accuracy	± 3 % NBS traceable absolute radiometric accuracy at 633 nm
Repeatability	± one digit.
Linearity	3 %
Output Impedance	10 kΩ
Analog Output BW	180 kHz
Detector Filter	O.D. 3 neutral density filter

4. Series PD30 Ultra High Speed Photodetector

Manufacturer	Opto-Electronics Inc. Oakville, Ont. Canada
Model	Series PD30-01 with PS30 Power Supply
Photodiode	avalanche-type silicon
Power Supply	200 μA current limited, variable voltage

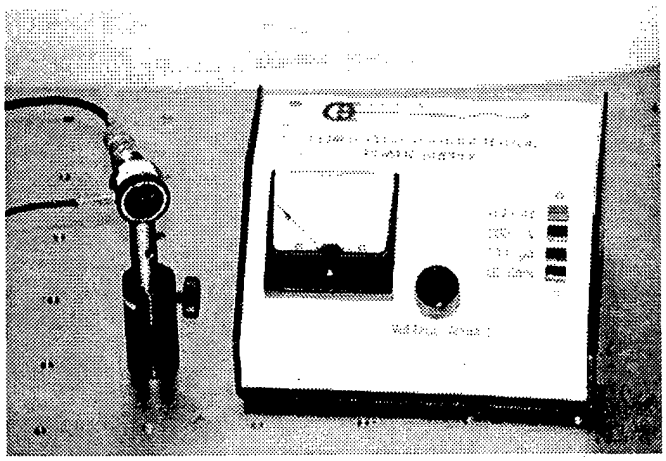

Figure C2. Photograph of Detector and Power Supply.

30-03 Serial number U016
Breakdown Voltage V_{BR}=136.6 VDC at 25°C
V_{max} = 138.1 VDC
FWHM 130ps observed
71.9 ps Source/Scope
<109 ps Detector with gain = 75
source wavelength 904 nm
do not exceed 100 mW average or 200 mW peak
power supply current gauge does not register until > 3 μW of laser power is incident on the detector at peak of sensitvity curve at 780 nm

5. Five Axis Alignment Platform

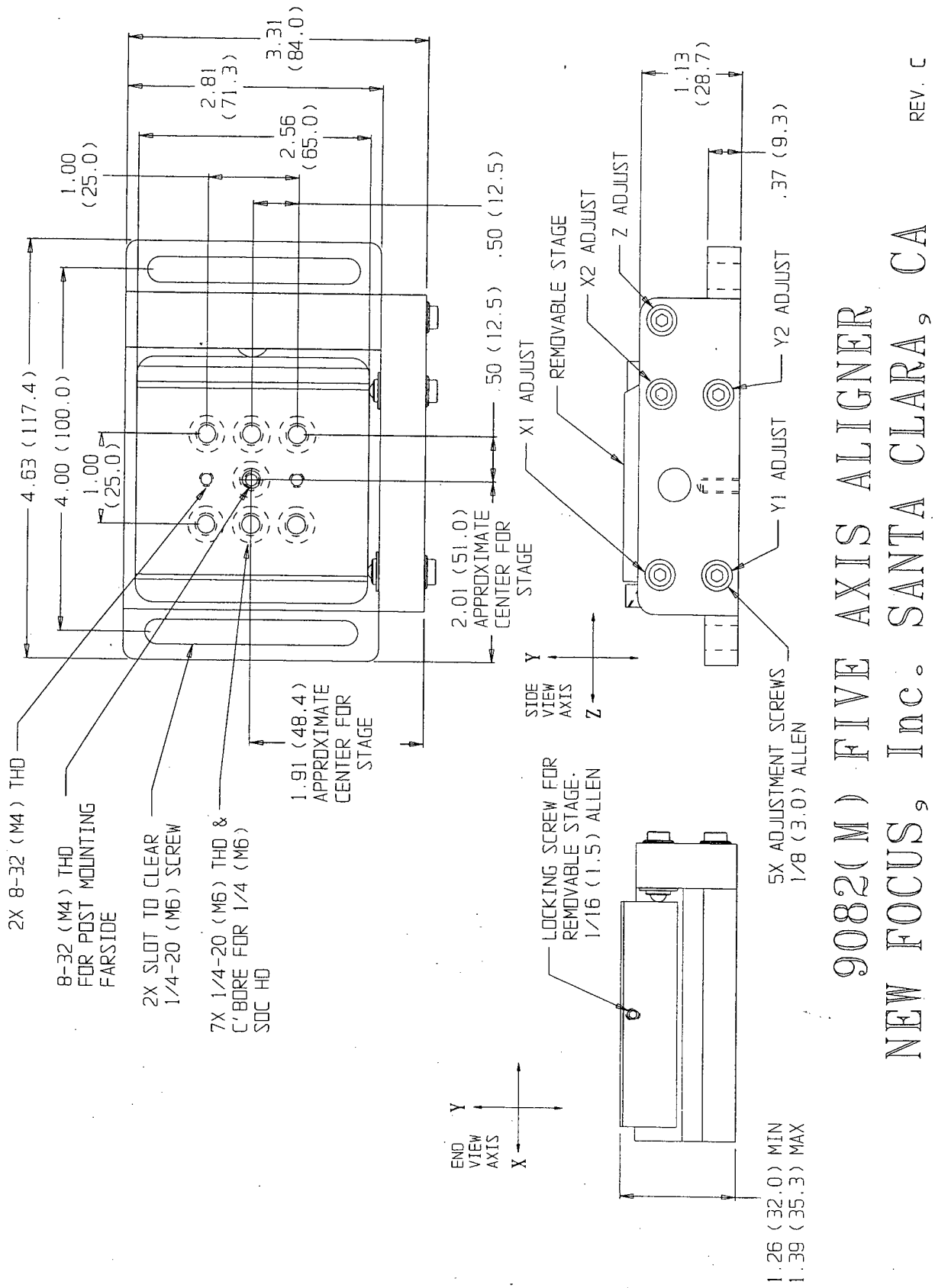

6. Mini-Circuits RF Amplifier

Manufacturer		Mini-Circuits Brooklyn, New York	
Model No.		TIA-1000-1R8	
Frequency		0.50 - 1000 MHz	
Gain	min	35 dB	
	flatness max	±2.0	
Max Power	output	typ	+35 dBm
		min	+32 dBm
	input	max	+7 dBm
Dynamic Range		NF	8* dB typ.
		IP3	45 dBm typ.
VSWR	In	1.9:1	
	Out	2.5:1	
AC Power	Volt	110	
	Freq	50/60 Hz	
	VA max	140	

Features
Aluminum alloy case
BNC connections
With no load, msx input (no damage) reduce by 10 dB

Freq (MHz) Gain (dB)

Frequency (MHz)	Gain (dB)	Directivity (dB)	VSWR in	VSWR out	NF (dB)	Pout (dBm)
0.5	40.65	56.72	1.42	2.84	-	36.10
12.6	40.48	58.36	1.20	1.36	17.34	36.62
99.5	40.98	50.05	1.23	2.26	14.13	36.19
207.6	40.33	51.07	1.27	2.61	10.29	34.61

Table C1. Manufacturer Performance Data.

*NF above 400 MHz. At low frequency, NF increases to 16 dB Typ.

LIST OF REFERENCES

1. Larraza and Coleman, *Nonlinear Propagation in Optical Fibers: Applications to Tunable Lasers*, Andres Larraza, paper prepared for thesis students.

2. J. Wilson and J.F.B Hawkes,*Optoelectronics, An Introduction, Second Edition*, Prentice Hall, Englewood Cliffs, New Jersey, 07632,1989.

3. *Application Note 3, Polarization and Polarization Control*, New Focus Inc., Sunnyvale, CA, 1996.

4. Amnon Yariv, *Introduction to Optical Electronics*, Holt, Rinehart and Winston, Inc., 1971.

5. *Application Note 2, Practical Uses and Applications of Electro-Optic Modulators*, New Focus Inc., Sunnyvale, CA., 1996.

6. Leonard S. Bobrow, *Fundamentals of Electrical Engineering*, Holt, Rinehart and Winston, Inc., 1985.

7. *Reference Data for Radio Engineers*, Fifth Edition, Howard W. Sams & Co., INC., 1968.

8. *Model 85 Ion Laser Operator Manual*, Cooper LaserSonics Inc., 1984.

INITIAL DISTRIBUTION LIST

1. Defense Technical Information Center 2
   8725 John J. Kingman Rd., STE 0944
   Ft. Belvoir, Virginia 22060-6218

2. Dudley Knox Library 2
   Naval Postgraduate School
   411 Dyer Rd.
   Monterey, California 93943-5101

3. Dr. W. B. Colson, Code PH/Co 1
   Department of Physics
   Naval Postgraduate School
   Monterey, California 93943-5002

4. Professor A. Larraza, Code PH/La 2
   Department of Physics
   Naval Postgraduate School
   Monterey, California 93943-5002

5. Professor S. Gnanalingham, Code PH/Gm 2
   Department of Physics
   Naval Postgraduate School
   Monterey, California 93943-5002

6. Professor Scott Davis, Code PH/Dv 2
   Department of Physics
   Naval Postgraduate School
   Monterey, California 93943-5002

7. Professor J. H. Luscombe, Code PH/Lj 1
   Department of Physics
   Naval Postgraduate School
   Monterey, California 93943-5002

8. Professor D. Walters, Code PH/We 1
   Department of Physics
   Naval Postgraduate School
   Monterey, California 93943-5002

9. LT Michael C. Ladner 2
   2350 South 2300 East
   Salt Lake City, UT 84109

10. LT Harlan Wallace.....2
4479 Camille St
Salt Lake City, UT 84124